

3-DIMENSIONAL MONTE CARLO SIMULATION  
OF LIPID-GRAMICIDIN A INTERACTION  
IN MODEL MEMBRANES

By

JIAN XING

Bachelor of Science

Sichuan University

Chengdu, Sichuan

People's Republic of China

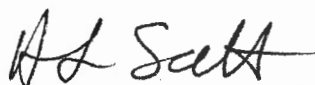
1982

Submitted to the Faculty of the  
Graduate College of the  
Oklahoma State University  
in partial fulfillment of  
the requirements for  
the Degree of  
MASTER OF SCIENCE  
July, 1989

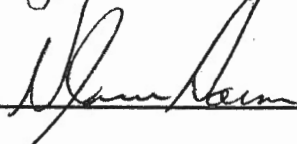
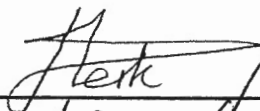
Thesis  
1989  
X 6<sup>+</sup>  
cop. 2

3-DIMENSIONAL MONTE CARLO SIMULATION  
OF LIPID-GRAMICIDIN A INTERACTION  
IN MODEL MEMBRANES

Thesis Approved:



\_\_\_\_\_  
Thesis Adviser



\_\_\_\_\_  
Dean of the Graduate College

## ACKNOWLEDGMENTS

I would first like to express my appreciation to Dr. H. L. Scott, my adviser, for his suggestion of the topic, and his invaluable guidance during this investigation and preparation of this thesis.

I wish to express my sincere gratitude to Dr. J. H. H. Perk and Dr. H. J. Harmon, the other members of my graduate committee, for their guidance and counseling. I wish to extend a special thanks to Dr. W. S. McCollough for his exceedingly helpful suggestions and comments on computer works.

I wish to express my thanks to Dr. P. A. Westhaus for much help during my graduate study here, and I also would like to express my thanks to everyone who has taught me or given me help in this department. I thank Ms. Yu-Mei Zhao for tracing most of the figures.

I wish to express my sincere appreciation to my parents for giving me guidance, support and strength throughout my life. I also wish to thank my father and mother-in-law for encouragement and assistance at all times. I wish to express my deepest thanks to my wife, Zhi Qin, for her many sacrifices, infinite patience and constant understanding. I wish this thesis will be a gift to all of them.

## TABLE OF CONTENTS

Chapter		Page
I.	INTRODUCTION . . . . .	1
	1-1 Conformational States of Lipids in Biomembranes . . . . .	1
	1-2 Gramicidin A - Phospholipid Model System . . . . .	7
	Conformation of Gramicidin A . . . . .	8
	Gramicidin A Transmembrane Channel . . . . .	10
	Phospholipid - Gramicidin A Interactions . . . . .	13
II.	THEORY . . . . .	14
	The Monte Carlo Method in Statistical Physics . . . . .	14
III.	METHODS . . . . .	17
	3-1 3-Dimensional Monte Carlo Simulation of Lipid-	
	Gramicidin A Interactions . . . . .	17
	Gramicidin Coordinate Input . . . . .	17
	Calculation of Initial Chain Configurations . . . . .	19
	Interaction Energy Calculations . . . . .	23
	Procedure for Saving Old Configurations and Energies . . . . .	25
	Procedure for Picking a Chain . . . . .	25
	Procedure for Whole Chain Translation . . . . .	25
	Procedure for Gauche Rotations . . . . .	25
	Procedure for Long-Axis Rotation . . . . .	29
	Periodic Boundary Conditions . . . . .	30
	Procedure for Change In Energy Calculations . . . . .	30
	Acceptance Criteria for Monte Carlo Moves . . . . .	30
	Procedure for Gramicidin A Configuration Changes . . . . .	30
	Procedure for Calculating Averages . . . . .	36
	3-2 Run Procedures . . . . .	38
IV.	RESULTS & DISCUSSION . . . . .	39
	4-1 Results . . . . .	39
	DMPC-Gramicidin A System . . . . .	39
	DPPC-Gramicidin A System . . . . .	42
	4-2 Discussion . . . . .	45
	BIBLIOGRAPHY . . . . .	52

Chapter	Page
APPENDIX A .....	55
APPENDIX B .....	56

Figure	LIST OF FIGURES	Page
1	Lipid-protein bilayer biomembrane model: the lipid molecules (A) form the bilayer; proteins (B) may totally ( $B_1$ ) or partially ( $B_2$ ) span the bilayer.(After Singer & Nicolson) . . . . .	2
2	Polymorphic phases: (a) planar lipid bilayer and (b) spherical lipid bilayer (vesicle); (c) micelles formed by lysophospholipids. . . . .	3
3	Two typical phospholipid molecules considered in this study: (a) DMPC (dimyristoyl phosphatidylcholine); (b) DPPC (dipalmitoyl phosphatidylcholine). . . . .	5
4	Configurations of a lipid chain: (a) all trans states; (b) one kink formed by two gauche rotations seperated by one trans bond; (c) jog formed by two or more gauche rotations separated by more than one trans bonds. . . . .	6
5	Schematic diagrams of models for the gramicidin A dimer: (A) amino-to-amino helical dimer; (B) carboxyl-to-carboxyl helical dimer; (C) antiparallel double helix; (D) parallel double helix. . . . .	9
6	Schematic representation of $\pi(L, D)$ type helices, showing approximately 6.3 residues per turn. . . . .	11
7	$\beta^{6.3}$ helical gramicidin dimer in a lipid bilayer: intramolecular hydrogen bonds are drawn as interrupted lines, intermolecular hydrogen bonds are drawn as <i>zig-zag</i> lines. . . . .	12
8	Flowchart of 3-dimensional Monte Carlo computer simulation for lipid-gramicidin A interactions. . . . .	18
9	A $10 \times 10$ array of carbon atoms representing the topmost atoms in each chain. . . . .	20
10	Generation of the positions of the hydrocarbon chain carbon atoms and carbon-carbon bonds: (a) configuration of lipid chain presented by Eq. $\vec{P}_{i+1} = \vec{P}_i + (ROT)\vec{R}_i$ ; (b) configuration of lipid chain performed by rotation ( $RT$ ). . . . .	21

Figure	Page
11 (a) Gauche rotations with (1) Gauche angle zero; (2) Gauche angle $+120^\circ$ ; (3) Gauche angle $-120^\circ$ ( $+240^\circ$ ). (b) The potential energy as a function of rotation angle. . . . .	26
12 Procedure for gauche rotations for bond $k$ : (a) $\rightarrow$ (b) for $k$ odd, the rotation operators are ( $ROT$ ) and ( $GR$ ); (a) $\rightarrow$ (c) $\rightarrow$ (d) $\rightarrow$ (e) for $k$ even, the rotation operators are ( $ROT$ ), ( $ROTP$ ), ( $GR$ ) and ( $ROTP$ ) $^{-1}$ . . . . .	28
13 Pictorial description of the chosen bond $k$ on a residue of gramicidin A: (a) location of the bond and the coordinate axes; (b) the relations of angle $A$ with angle $C'$ ; (c) the pictorial description for the derivation of $\sin C'$ . . . . .	32
14 The relations of angle $A$ with angle $C$ corresponding to the eight octants in the Cartesian system. . . . .	33
15 Pictorial procedure of the rotations around the chosen bond $k$ on a residue of gramicidin A with rotation operators ( $R_x^a$ ), ( $R_z^a$ ), ( $R_y^\theta$ ), ( $R_z^a$ ) $^{-1}$ and ( $R_x^a$ ) $^{-1}$ . . . . .	35
16 The relations between bond angles $\theta_n^\circ$ , $\theta'_n$ and $\theta_n$ : $\theta_n^\circ$ is the original angle; $\theta'_n$ is the new angle; $\theta_n$ is the deviation. . . . .	37
17 Order-parameter profile $\langle S_n \rangle$ vs bond number $n$ for calculated averages from DMPC (C-14) simulations: ( $\Delta$ ) average for all chains; (*) average for nearest-neighbor chains of gramicidin A; (o) experimental data from $^2\text{H-NMR}$ . . . . .	40
18 Size comparison of gramicidin A with DMPC and DPPC chains. . . . .	41
19 Top view and side view of a typical configuration of gramicidin A and its neighboring chains ( DMPC ) after 60,000 MC steps: (a) top view; (b) side view. . . . .	43
20 Order-parameter profile $\langle S_n \rangle$ vs bond number $n$ for calculated averages from DPPC (C-16) simulations: ( $\Delta$ ) average for all chains; (*) average for nearest-neighbor chains of gramicidin A; (o) experimental data from $^2\text{H-NMR}$ . . . . .	44
21 Top view and side view of a typical configurations of gramicidin A and its neighboring chains ( DPPC ) after 60,000 MC steps (a) top view; (b) side view. . . . .	46



Figure		Page
22	Experimental data from $^2\text{H}$ -NMR; (a') shows the orderparameter profile $S_n$ corresponding to (a). Taken from Rice and Oldfield [33] . . . . .	48

LIST OF TABLES

Table		Page
I	STANDARD DEVIATIONS OF $\langle S_n \rangle$ FOR DMPC DATA . . . .	50
II	STANDARD DEVIATIONS OF $\langle S_n \rangle$ FOR DPPC DATA . . . .	51

## CHAPTER I

### INTRODUCTION

For a number of years there has been much interest in developing and applying physical methods, experimentally or theoretically, to study the structure of biological membranes. It is generally known that biological membranes are made up of a variety of phospholipid molecules and membrane proteins (Fig. 1). Therefore lipid-lipid interaction and lipid-protein interaction in membranes has been an active field of study on a number of levels. Because biological membranes are highly heterogeneous in their molecular composition, much attention is focused on artificially synthesized model membranes in which the composition may be controlled by the experimenter. Model membranes have been studied by various experimental techniques such as X-ray diffraction, electron spin resonance (ESR), differential scanning calorimetry (DSC), nuclear magnetic resonance (NMR) etc., and by theoretical and numerical methods.

#### 1-1 Conformational States of Lipids in Biomembranes

The early X-ray diffraction studies [22] firmly established the fact that the lipids in biological membranes are predominantly organized in bilayer structures and that the average orientation of the hydrocarbon chains of the lipids is perpendicular to the lipid-water interface. Biological lipids, such as phosphatidylcholine, sphingomyelin, phosphatidylserine and phosphatidylglycerol, dispersed in aqueous solution, will spontaneously form biomolecular bilayers, which may be planar or spherical (vesicle). The single-tail soaps, such as lysophospholipids, tend to form small spherical structures in water, called micelles [27](see Fig. 2). The

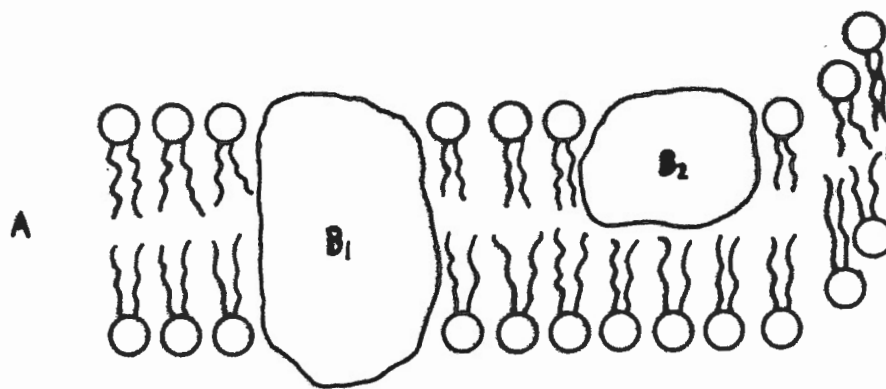


Figure 1. Lipid-protein bilayer biomembrane model: the lipid molecules (A) form the bilayer; proteins (B) may totally (B<sub>1</sub>) or partially (B<sub>2</sub>) span the bilayer. (After Singer & Nicolson).

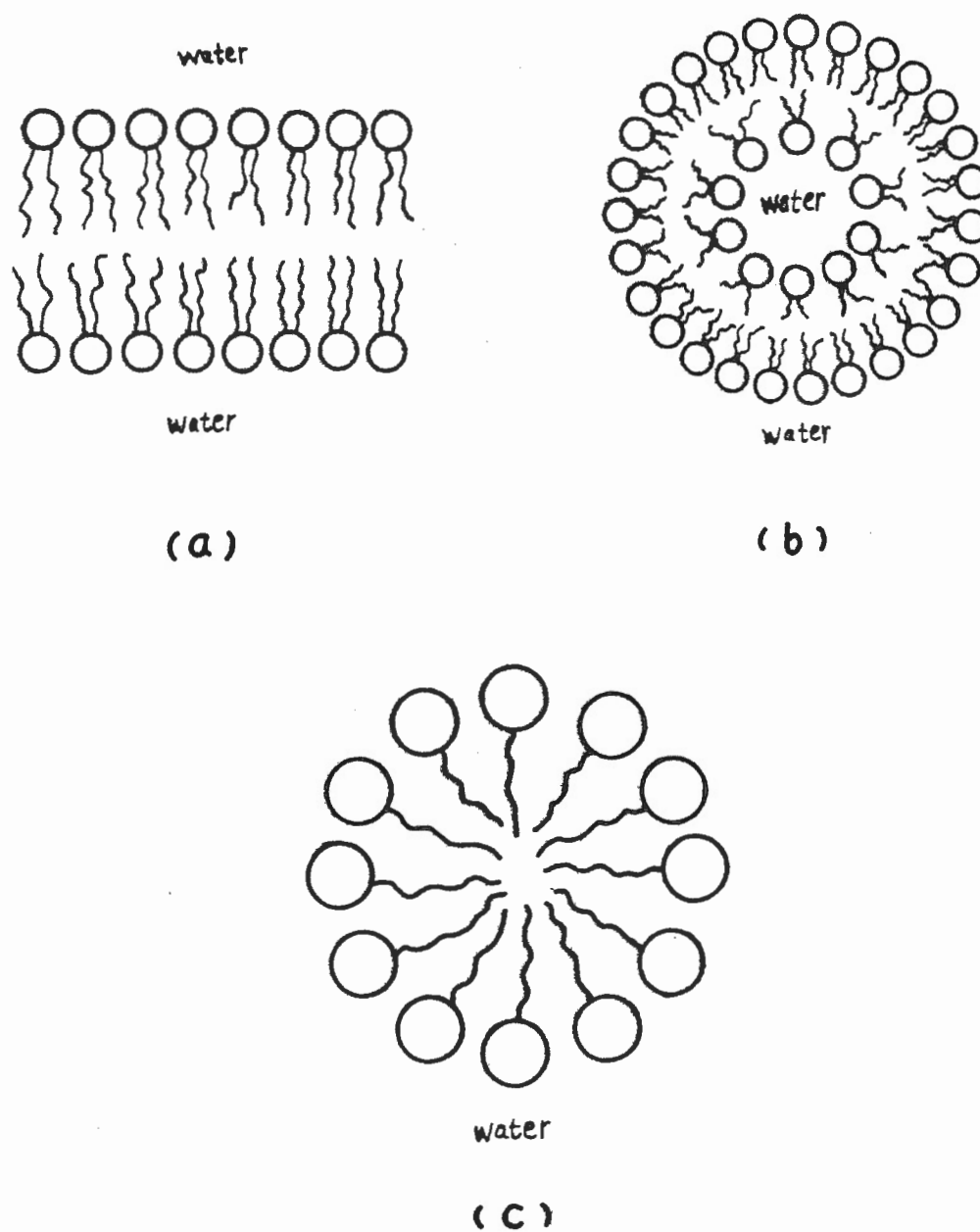


Figure 2. Polymorphic phases: (a) planar lipid bilayer and (b) spherical lipid bilayer (vesicle); (c) micelles formed by lysophospholipids.

lipid molecules in a planar or spherical membrane bilayer have their hydrophilic polar head groups located at the aqueous interfaces of the bilayer, and their hydrophobic (water fearing) tails in the center of the bilayer. This structure results in two regions, a hydrophilic portion at the outside of the biomembrane in which the polar groups of the amphiphilics interact with water molecules, and a hydrophobic region in the interior region. A major problem of interest is the chain packing problem, which includes static aspects, such as the average overall chain conformations and interaction strengths, and dynamic aspects, such as the rotational, translational and conformational mobility of the chains in the restricted volume. Scott *et al.* have studied the lipid chain packing in bilayers and micelles using Monte Carlo methods [36, 37, 38, 39], [27] and [14]. By means of  $^2\text{H}$ -NMR Seelig *et al.* have experimentally studied the lipid chain conformations in biomembranes [42, 43, 44, 45]. A clear view of the nature of the conformations of lipid chains in biological membranes and model membranes has resulted from these and other studies.

There are a wide variety of lipids in biomembranes. Two typical phospholipids, which will be simulated in this study, are : (a) DMPC (dimyristoyl phosphatidylcholine) and (b) DPPC (dipalmitoyl phosphalidylcholine) (see Fig. 3). These molecules have saturated carbon-carbon bonds of length 1.53 Å. The molecular conformations may change via gauche rotations around the carbon-carbon bonds. It is a good approximation to consider only three rotational states [42] : a trans (t) configuration at the dihedral angle  $\phi_i = 0^\circ$  and two gauche configurations ( $g^+$  and  $g^-$ ) at  $\phi_i = +120^\circ$  and  $-120^\circ$ . Fig. 4 shows how these states are associated with the conformation of a whole lipid chain. At low temperature, the conformations of the lipid chain are all trans because this state has the lowest energy, and the thickness of the bilayer is greatest. With the alteration of temperature, water content, ion concentration, lipid composition, and various other parameters, the conformation of lipid chains may change from a more rigid gel phase to a more fluid liquid-crystalline phase, in which the chains undergo rapid reorientation, including

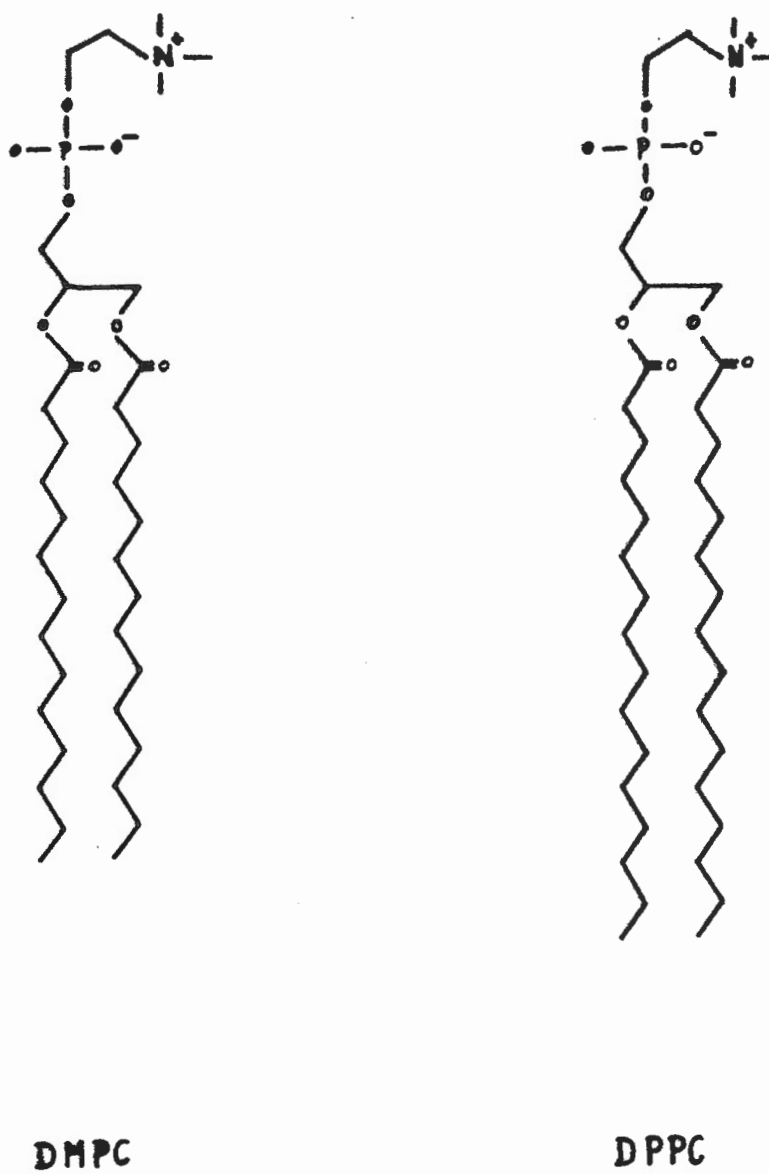


Figure 3. Two typical phospholipid molecules considered in this study:  
(a) DMPC (dimyristoyl phosphatidylcholine); (b) DPPC (dipalmitoyl phosphatidylcholine).

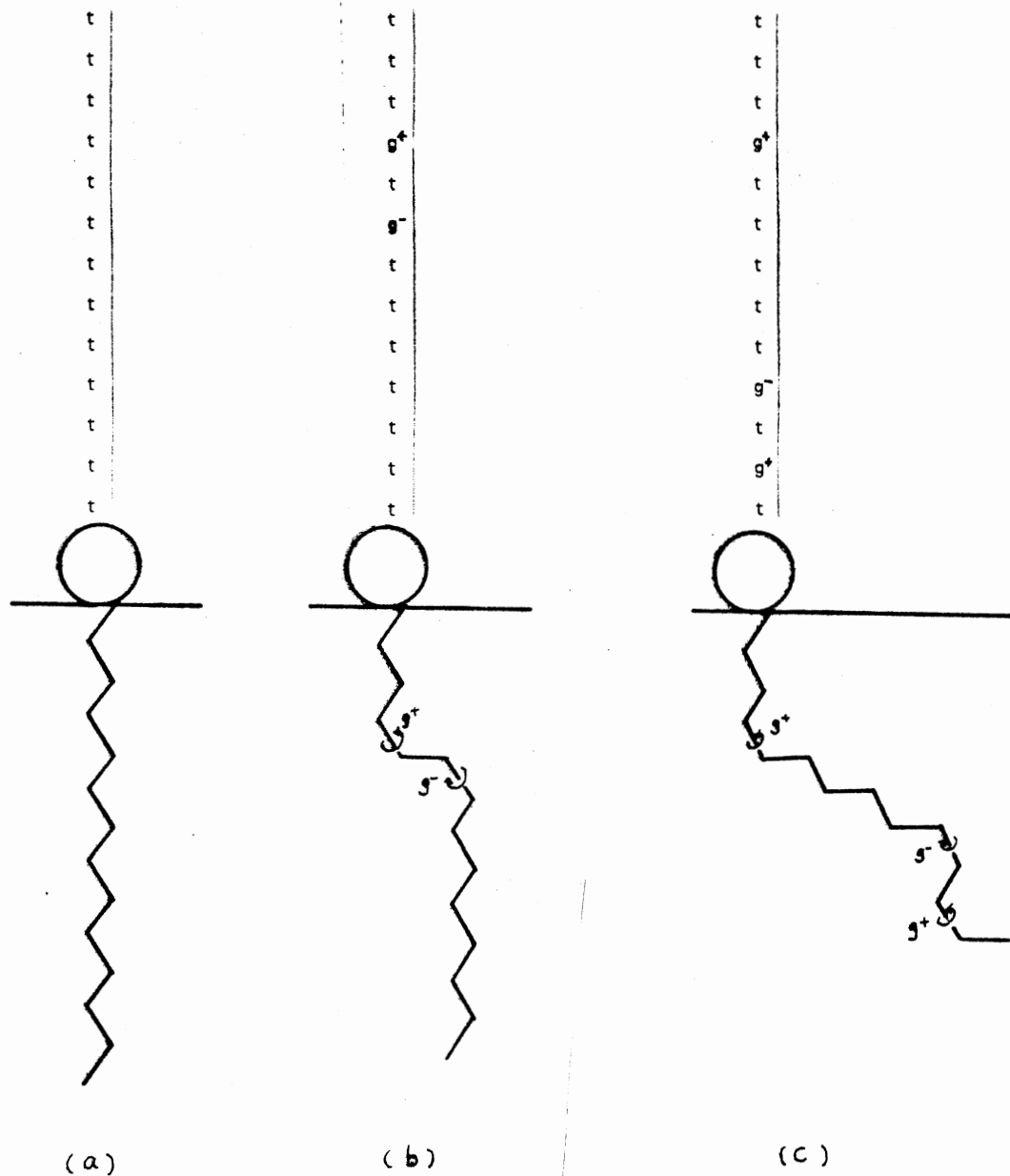


Figure 4. Configurations of a lipid chain: (a) all trans states; (b) one kink formed by two gauche rotations separated by one trans bond; (c) jog formed by two or more gauche rotations separated by more than one trans bonds.



trans-gauche segmental rotations and lateral molecular diffusion, as well as slower motions, such as collective chain tilting and molecular long axis rotation [39].

For lipid chains in a bilayer the conformational states of lipids are determined by the available thermal energy and by the intermolecular interactions. These interactions include van der Waals attractions, which pull the hydrocarbon chains towards each other, and steric repulsion, which prevent the overlap of molecules within a hard core radius.

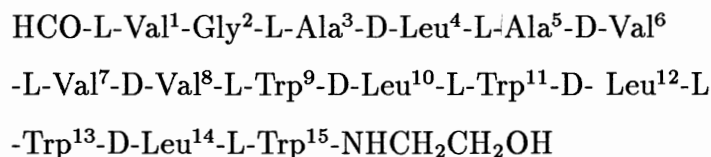
Order parameters often provide a convenient way to describe the average conformations of the hydrocarbon chains. They are directly obtained from deuterium-NMR [46] experiments, and may be readily calculated in numerical simulations. The order parameter for bond number  $n$  on a hydrocarbon chain is defined by :

$$\langle S_n \rangle = (1/2) \langle 3 \cos^2 \theta_n - 1 \rangle \quad (1)$$

where  $\theta_n$  is the angular deviation of bond  $n$  from its original orientation in the all-trans state. Calculated profiles of  $\langle S_n \rangle$  vs  $n$  will be described in *Chapters 3* and *4*.

### 1-2 Gramicidin A - Phospholipid Model System

Since Hotchkiss published his study of gramicidin [13], a colorless crystal, soluble in organic solvents and isolated from cultures of bacillus brevis, a number of scientists have been very interested in this antibiotic. The first definitive study of the chemical structure of gramicidin A was published by Sarges and Witkop [34]. They used gas chromatography and thin layer chromatography to get the chemical structure of gramicidin A :



Gramicidin A is therefore a linear polypeptide antibiotic consisting of 15 hydrophobic amino acids of alternating L and D configuration (see Appendix A for more detail).

Much of the current research involving gramicidin A may be grouped into three areas :

1. the conformation of gramicidin A in the crystalline structure and in a membrane;
2. the kinetics of facilitated ion conduction across a lipid membrane by gramicidin A;
3. the interaction of gramicidin A with its supporting lipid membrane.

It should be pointed out that the three areas are strongly associated with each other. For example, in order to study the interaction of gramicidin A with lipid membrane, the conformation of gramicidin A in the membrane must be known.

### Conformation of Gramicidin A

Gramicidin A is a member of the gramicidin family that includes gramicidin A, B, C and D, which predominantly differ from each other in the amino acid group at position 11 (tryptophan, gramicidin A; phenylalanine, gramicidin B; tyrosine, gramicidin C). The conformation of gramicidin A depends on its environment. The conformations are different for gramicidin A in a single crystal, in solution, or in a membrane.

A neutron diffraction study to 5 Å resolution of an ion-free crystal of gramicidin A, reported by Koeppel and Schoenborn [19], yielded helical dimers resembling parallel 32-Å-long cylinders (see Fig. 5 D). However, a double-stranded antiparallel  $\uparrow\downarrow \beta^{5.6}$  which is  $\beta$  helix with 5.6 residues per turn (see Fig. 5 C) was found by Naik and Krimm [29] based upon theoretical analysis of vibrational spectra. Wallace [50] reported studies of the three-dimensional structure of a gramicidin/cesium complex by X-ray diffraction of single crystals.

Gramicidin A is virtually insoluble in water. Convenient solvents for gramicidin A include dimethyl sulfoxide, methanol, ethanol, ethyl acetate, acetone, chloroform, benzene, and dioxane. The conformation of gramicidin A in a dioxane solvent system has been determined by Arseniev et al. [3] using two-dimensional

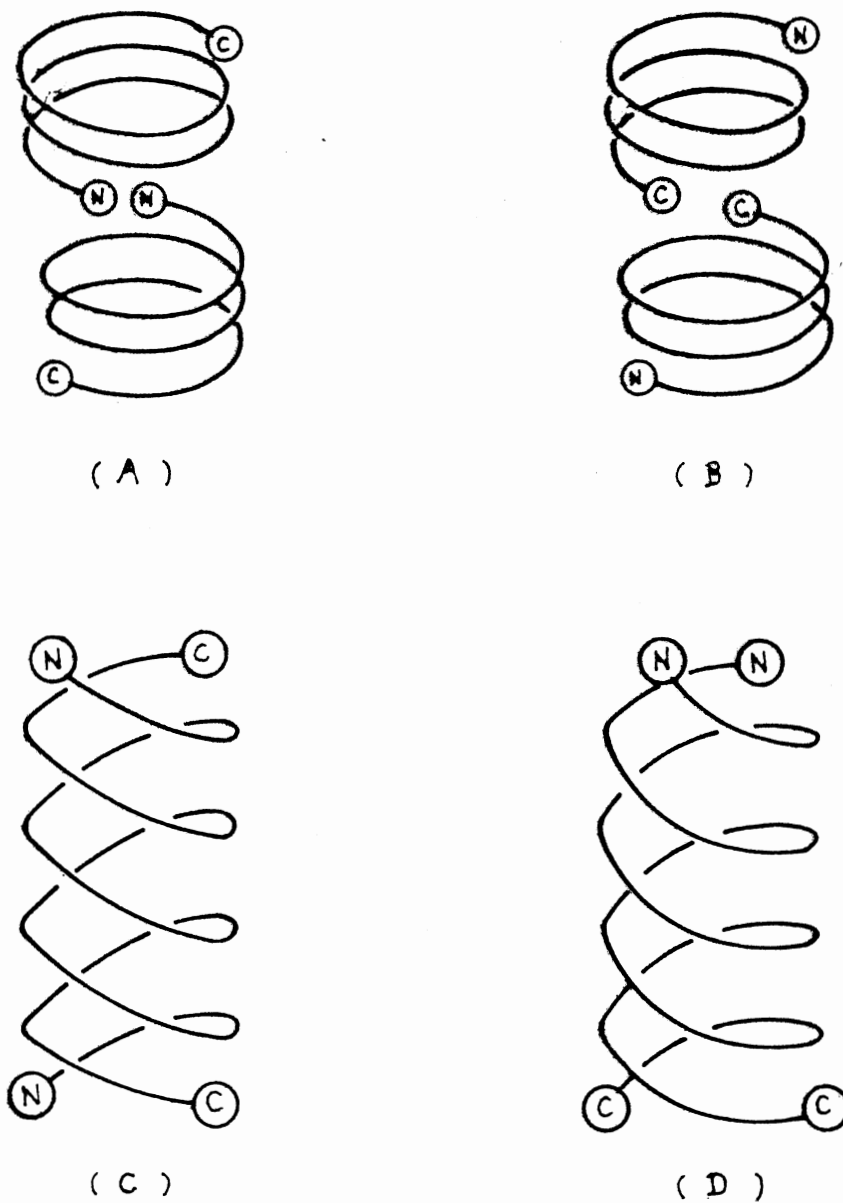


Figure 5. Schematic diagrams of models for the gramicidin A dimer: (A) amino-to-amino helical dimer; (B) carboxyl-to-carboxyl helical dimer; (C) antiparallel double helix; (D) parallel double helix.

$^1\text{H-NMR}$ , to get the left-handed antiparallel double helix with 5.6 residues per turn, denoted by ( $\uparrow\downarrow \beta_{L,D}^{5.6}$ ) (see Fig. 5 C).

For gramicidin in lipid bilayers, Naik and Krimm used normal model analysis to reach the conclusion that the single-stranded helix with 6.3 residues per turn  $\beta^{6.3}$  is the more likely structure [28, 29]. This result supports the earlier studies reported by Urry et al. [47], which described the conformation of gramicidin A in lipid bilayer as a left-handed  $\pi(\text{L.D})$  helix with 6.3 residues per turn (or denoted by  $\beta^{6.3}$ -helix) (see Fig. 6), with two helices form a transmembrane channel by head-head dimer(see Fig. 5 A).

At present, the conformation of gramicidin A in a lipid bilayer is generally thought to be a  $\beta^{6.3}$  helix [6, 49, 51, 52, 18, 8, 5], although the handedness remains in doubt (a right-handed, single-stranded  $\beta^{6.3}$  helix was reported by Arseniev et al. [4]).

### Gramicidin A Transmembrane Channel

As discussed above, the gramicidin A transmembrane channel is the  $\beta^{6.3}$  helix dimer. In this conformation the channel has a luminal diameter of 4 Å, a length of about 26 Å and with a helical pitch of 4.8 Å. The two single-stranded  $\beta^{6.3}$  helices are stabilized by 6 intermolecular and 22 intramolecular hydrogen bonds [31](Fig. 7). The wall of a gramicidin channel is lined by the polar groups in the peptide backbone. These polar groups form an array of coordination sites (associated with the carbonyl oxygens) along the axis of the helix. The peptide groups interact with the permeating ions and water molecules to decrease the energy barrier for ion movement through the channel. The permeability characteristics of the channel are determined by the characteristics of the polar permeation path as well as its narrow and uniform lumen. Andersen et al. [1] pointed out that the magnitude of the single-channel conductance is primarily determined by the polar backbone (carbonyl oxygens), and also depends on the amino acid sequence (different kinds of residues). Alterations (changes of the polar head or the thickness of bilayer) of the composition of the bilayer result in the changes of the permeability

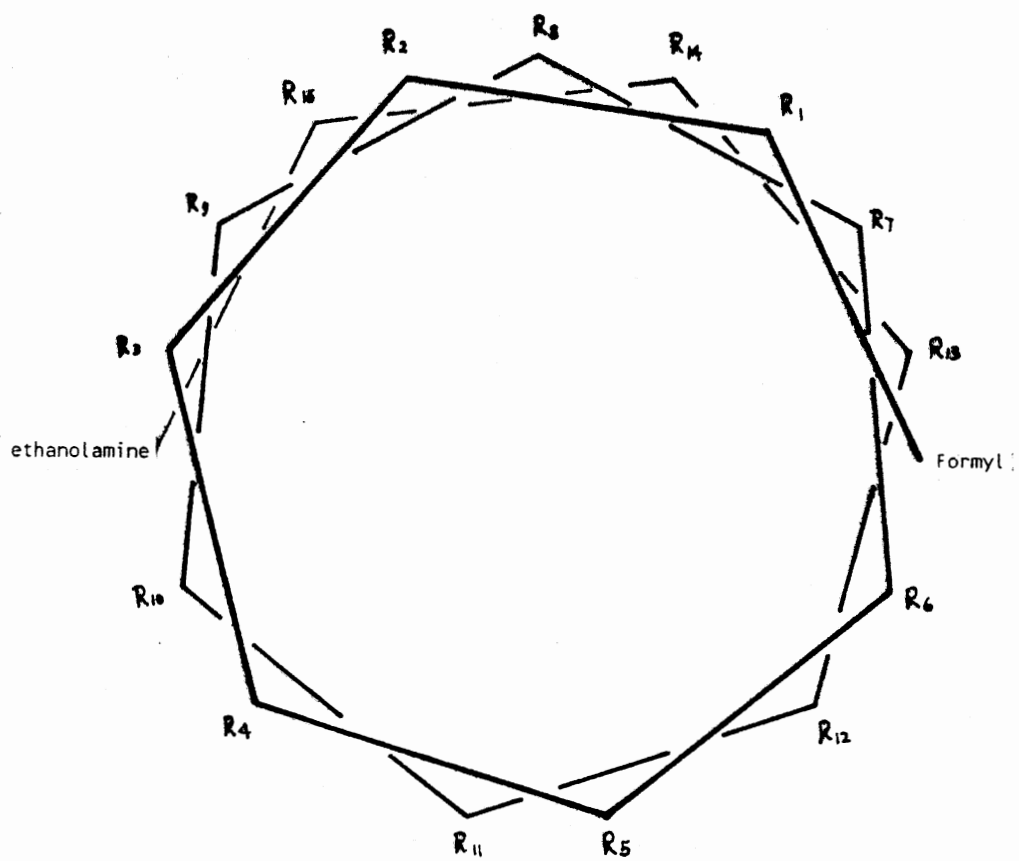


Figure 6. Schematic representation of  $\pi(L, D)$  type helices, showing approximately 6.3 residues per turn.

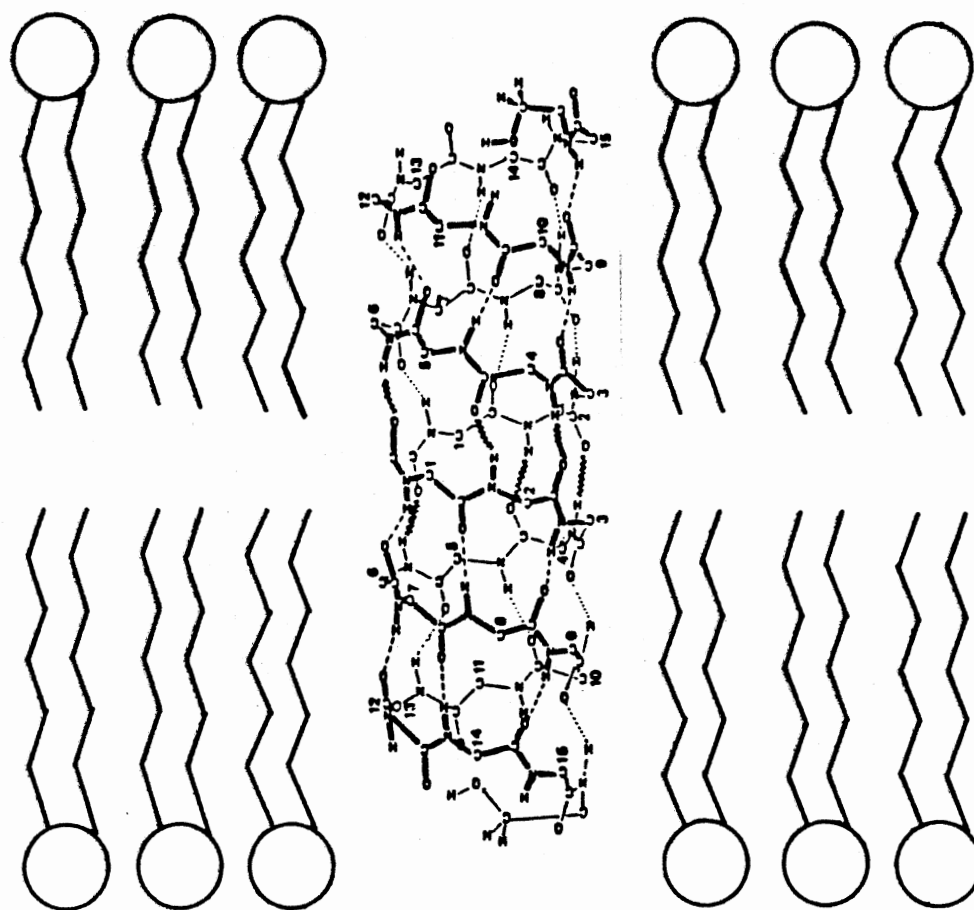


Figure 7.  $\beta^{6.3}$  helical gramicidin dimer in a lipid bilayer:  
intramolecular hydrogen bonds are drawn as interrupted  
lines, intermolecular hydrogen bonds are drawn as *zig-*  
*zag* lines.

of the gramicidin channel. Neher and Eibl [30] have studied the influence of phospholipid polar groups on gramicidin channels and concluded that the conductance changes could result from the changes in the polar head group of phospholipids alone. Kolb and Bamberg [20] have studied the influence of membrane thickness on the properties of the gramicidin A channel. The result indicates that the conductance changes also result from the changes in the fatty acid composition of phospholipids with identical head groups.

### Phospholipid - Gramicidin A Interactions

We have mentioned the effects of phospholipids on gramicidin A in the above section. At the same time there are effects of gramicidin A on the phospholipids. These interactions are determined by various conditions such as the polar head of phospholipids, bilayer thickness, the concentration of gramicidin and the temperature.

Lee et al. [21] reported difference infrared spectroscopic studies of DMPC-gramicidin, which indicated partial ordering of the lipid chains by gramicidin above the pure lipid transition temperature. Below the transition, gramicidin was observed to partially disorder the lipid chains, which means addition of gramicidin A to DMPC bilayers broadened the phase transition but did not significantly shift the transition temperature. This result was supported by the reports of Macdonald et al. [23]. Independently, using differential scanning calorimetry (DSC) and  $^2\text{H}$ -NMR, Morrow et al. [25] reported a broadening of the peak in the excess heat capacity at the lipid phase transition and the downward shift in transition temperature of lipids relative to the transition temperature of pure lipid bilayer is approximately 3 °C for DMPC-gramicidin system and 4 °C for DPPC-gramicidin system. ESR studies [16, 17, 12] have suggested that a protein-containing bilayer lipid is far more ordered than a protein-free bilayer.

The purpose of this thesis is to report the results of a 3-dimensional Monte Carlo computer simulation for DMPC-gramicidin A and DPPC-gramicidin A systems.

## CHAPTER II

### THEORY

This research is based on the application of statistical physics to the study of lipid-lipid and lipid-protein interaction in model biomembranes. In this chapter the general Monte Carlo method will be described.

#### The Monte Carlo Method in Statistical Physics

The Monte Carlo method was introduced by Metropolis et al.[24]. It consists of a biased sampling of the phase space of a system of many particles, and under certain circumstances it will correctly predict the thermodynamic properties of the system.

Consider a system of  $N$  particles in a volume  $V$  at temperature  $T$ . The total potential energy of the system may be written as

$$E = \frac{1}{2} \sum_{i=1}^N \sum_{j=1}^N V(r_{i,j}) \quad (2)$$

where,  $r_{i,j}$  is the distance between particle  $i$  and particle  $j$  and  $V$  is the potential energy between molecules.

In the canonical ensemble, the thermodynamic average of any observable quantity  $A(q, p)$  has the form

$$\langle A \rangle = \frac{\int_{\Omega} A(p, q) e^{-E(p, q)/kT} d^{3N} p d^{3N} q}{\int_{\Omega} e^{-E(p, q)/kT} d^{3N} p d^{3N} q} \quad (3)$$

where  $\Omega$  is the phase space of system,  $k$  is the Boltzmann constant.

For the Monte Carlo method, the integral of Eq. (3) is evaluated by a random sampling of points selected according to a probability  $P(\mu)$ , instead of over a regular array of points, in phase space  $\Omega$ . In this case, Eq. (3) can be written as [7]

$$\langle A \rangle = \frac{\sum_{\mu=1}^M A(\mu) e^{-E_{\mu}/kT} / P(\mu)}{\sum_{\mu=1}^M e^{-E_{\mu}/kT} / P(\mu)} \quad (4)$$



where  $1/P(\mu) \propto N(\mu)$ , the number of configurations having energy  $E(\mu)$ . At thermal equilibrium  $P(\mu) = \text{constant} \cdot e^{-E_\mu/kT}$ , so, we get

$$\langle A \rangle = \frac{1}{M} \sum_{\mu=1}^M A(\mu) \quad (5)$$

where  $M$  is the total number of configurations (total number of phase states).  $A(\mu)$  can be any observable quantity when the system is in configuration  $\mu$ .

The random walk through phase space must be defined so that in equilibrium  $P_{eq}(\mu) \sim e^{-E_\mu/kT}$ . This is done in the following manner : Let  $W$  be the transition probability per unit time from configuration  $\mu$  to configuration  $\mu'$  in the phase space of the system. The first derivative of  $P(\mu)$  with respect to time  $t$  can be written as

$$\frac{dP(\mu)}{dt} = - \sum_{\mu} W_{\mu \rightarrow \mu'} P(\mu) + \sum_{\mu'} W_{\mu' \rightarrow \mu} P(\mu') \quad (6)$$

We must construct a random walk through phase space via a Markov process, such that  $P(\mu)$  tends towards  $P_{eq}(\mu)$  as the total number of steps  $M$  is sufficiently large [7]. In equilibrium the left hand side of Eq. (6) is zero, so

$$W_{\mu \rightarrow \mu'} P_{eq}(\mu) = W_{\mu' \rightarrow \mu} P_{eq}(\mu') \quad (7)$$

Since  $P_{eq}(\mu) \propto e^{-E_\mu/kT}$ ,

$$\frac{W_{\mu \rightarrow \mu'}}{W_{\mu' \rightarrow \mu}} = \frac{P_{eq}(\mu')}{P_{eq}(\mu)} = e^{-(E_{\mu'} - E_\mu)/kT} = e^{-\Delta E_{\mu \rightarrow \mu'}/kT} \quad (8)$$

Now we choose  $W_{\mu \rightarrow \mu'}$  (this choice is not unique [26])

$$W_{\mu \rightarrow \mu'} \propto \begin{cases} 1 & \Delta E_{\mu \rightarrow \mu'} \leq 0 \\ e^{-\Delta E_{\mu \rightarrow \mu'}/kT} & \Delta E_{\mu \rightarrow \mu'} > 0 \end{cases} \quad (9)$$

With the choice Eq. (8) is always satisfied. In terms of the random walk through phase space, Eq. (9) means :

If  $\Delta E_{\mu \rightarrow \mu'} \leq 0$ , we accept the move ; If  $\Delta E_{\mu \rightarrow \mu'} > 0$ , according to the probability  $W_{\mu \rightarrow \mu'}$  in Eq. (9), we accept the move for  $e^{-\Delta E_{\mu \rightarrow \mu'}/kT} \geq x$  or reject the move for  $e^{-\Delta E_{\mu \rightarrow \mu'}/kT} < x$ , where  $x$  is a random number distributed uniformly on  $[0, 1]$ .

We continue this process for a very large number  $M$  of steps. In the limit  $M \rightarrow \infty$ ,  $\langle A \rangle$  converges to the values one would obtain from the exact calculation of the integral in Eq. (3).

## CHAPTER III

### METHODS

This research simulates a  $10 \times 10$  lipid-chain array with  $n$  carbon atoms ( $14 \leq n \leq 16$ ) per chain, and one gramicidin A monomer in the center of the array. In this chapter the numerical methods used in the simulation will be described. In *section 3-1* the flowchart for the program will be given, and each step will be described in detail. In *Section 3-2* the procedures used in running the program will be described.

#### 3-1 3-Dimensional Monte Carlo Simulation of Lipid-Gramicidin A Interactions

The flowchart of the computer program, which includes one main program and four subprograms, is shown in Fig. 8. The various steps shown in the flowchart will now be described in turn. First, we describe the coordinate system used in all simulations.

#### Gramicidin Coordinate Input

In the initial steps of the program, the gramicidin A monomer co-ordinates of Jakobsson ( private communication ) are read, and the monomer is positioned in the center of the simulation cell, with the alpha carbon of the tryptophan-15 residue in the bilayer plane. After any cycle of the program, the conformation of gramicidin A is generally changed due to residue rotations. In each subsequent run, therefore, the program reads the gramicidin A configuration from the previous run.

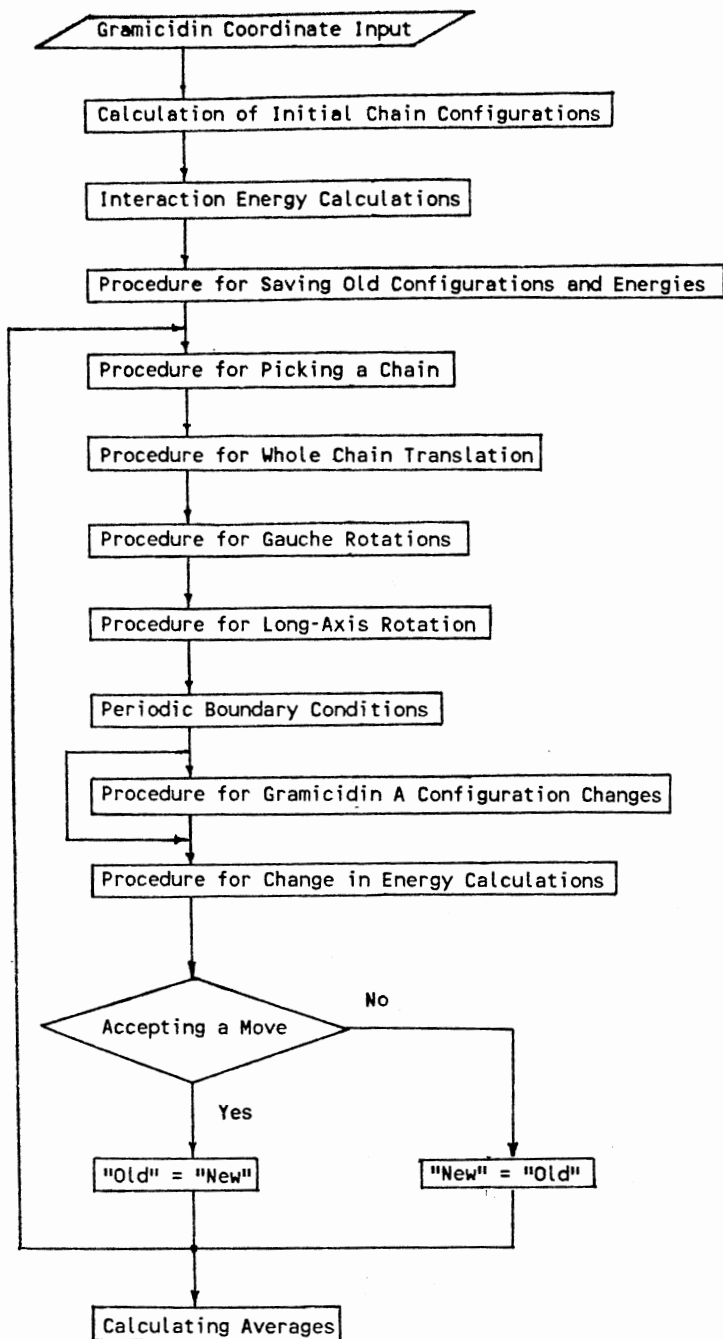


Figure 8. Flowchart of 3-dimensional Monte Carlo computer simulation for lipid-gramicidin A interactions.

### Calculation of Initial Chain Configurations

The method of generating the positions of the hydrocarbon chain carbon atoms is that of Scott and co-workers [40]. The procedure is as follows : First, a  $10 \times 10$  array of carbon atoms representing the topmost atoms in each chain is constructed in the  $Z - X$  plane (see Fig. 9). After removal of 6 chains to accommodate the gramicidin A, there actually are 94 chains in this model.

All the lengths of carbon-carbon bonds in lipids chain are held fixed at  $1.53 \text{ \AA}$  and bond angles are  $70.5^\circ$  as shown in Fig. 10. Let the position of the first carbon atom of a chain be given by

$$\vec{P}_1 = \begin{pmatrix} x \\ 0 \\ z \end{pmatrix}, \quad (10)$$

and the first C-C bond vector is

$$\vec{R}_1 = \begin{pmatrix} 0 \\ b \\ 0 \end{pmatrix}, \quad (11)$$

where  $b = 1.53 \text{ \AA}$ . Then, the positions of the second carbon  $\vec{P}_2$ , the third carbon  $\vec{P}_3$ , ... the  $(i + 1)$ th carbon  $\vec{P}_{i+1}$ , etc., are first calculated as

$$\vec{P}_2 = \vec{P}_1 + (ROT)\vec{R}_1, \quad (12)$$

$$\vec{P}_3 = \vec{P}_2 + (ROT)\vec{R}_2, \quad (13)$$

$$\dots = \dots, \quad (14)$$

$$\vec{P}_{i+1} = \vec{P}_i + (ROT)\vec{R}_i, \quad (15)$$

where  $\vec{R}_i = (ROT)\vec{R}_{i-1}$  for  $i > 1$  and  $\vec{R}_1$  is given by Eq. (11) The rotation operator  $(ROT)$  is actually a rotation about the  $Z$ -axis and a reflection about the  $X$ -axis given by

$$(ROT) = \begin{pmatrix} \cos \alpha_1 & \sin \alpha_1 & 0 \\ -\sin \alpha_1 & \cos \alpha_1 & 0 \\ 0 & 0 & 1 \end{pmatrix} \begin{pmatrix} -1 & 0 & 0 \\ 0 & 1 & 0 \\ 0 & 0 & 1 \end{pmatrix}, \quad (16)$$

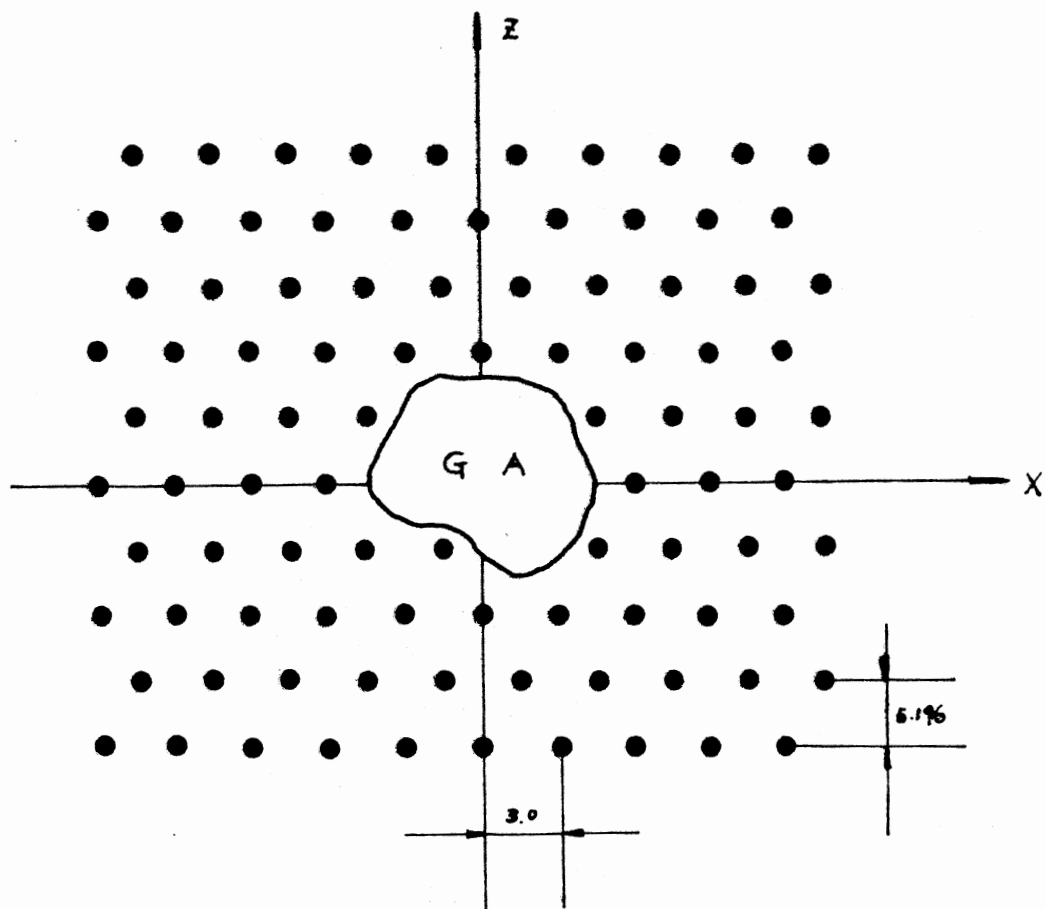


Figure 9. A  $10 \times 10$  array of carbon atoms representing the topmost atoms in each chain.

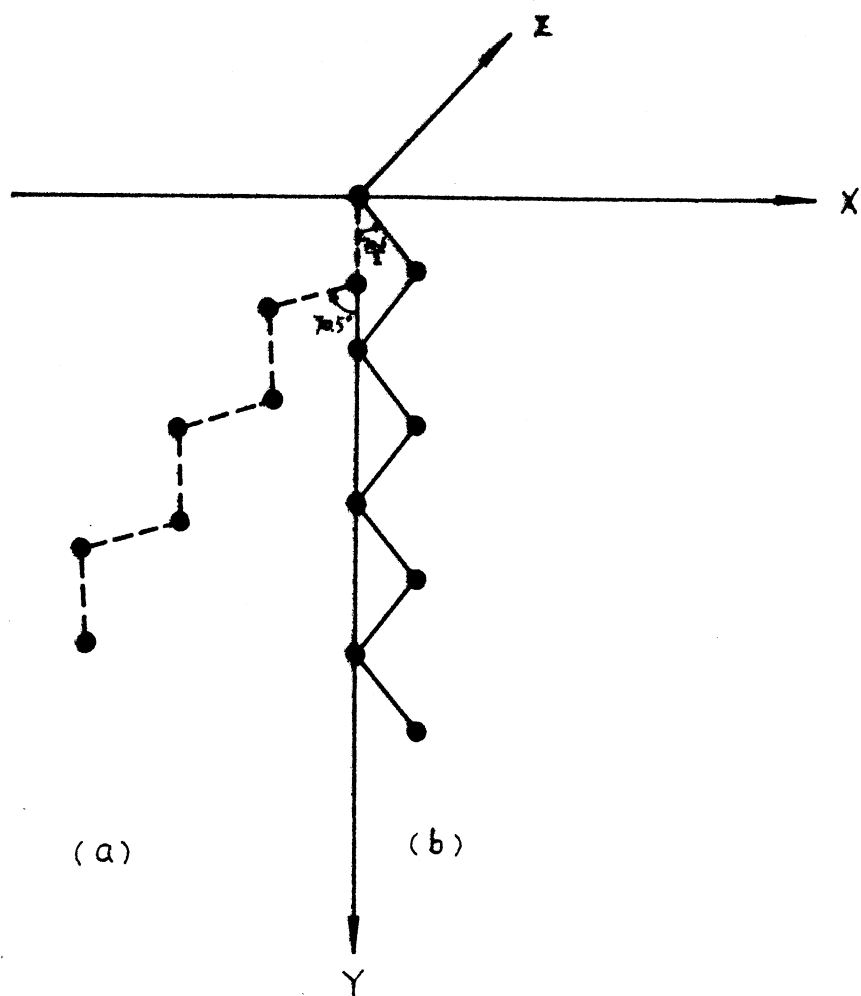


Figure 10. Generation of the positions of the hydrocarbon chain carbon atoms and carbon bonds: (a) configuration of lipid chain presented by Eq.  $\vec{P}_{i+1} = \vec{P}_i + (ROT)\vec{R}_i$ ; (b) configuration of lipid chain performed by rotation ( $RT$ ).

so,

$$(ROT) = \begin{pmatrix} -\cos \alpha_1 & \sin \alpha_1 & 0 \\ \sin \alpha_1 & \cos \alpha_1 & 0 \\ 0 & 0 & 1 \end{pmatrix} \quad (17)$$

where the angle  $\alpha_1 = 70.5^\circ$ . Thus it can be seen that the successive bond vectors of the chain are produced by successive rotation and reflection operations.

Substitute  $(ROT)$  into Eq. (12),

$$(ROT)\vec{R}_1 = \begin{pmatrix} -\cos \alpha_1 & \sin \alpha_1 & 0 \\ \sin \alpha_1 & \cos \alpha_1 & 0 \\ 0 & 0 & 1 \end{pmatrix} \begin{pmatrix} 0 \\ b \\ 0 \end{pmatrix} = \begin{pmatrix} b \sin \alpha_1 \\ b \cos \alpha_1 \\ 0 \end{pmatrix} = \vec{R}_2, \quad (18)$$

$$(ROT)\vec{R}_2 = \begin{pmatrix} -\cos \alpha_1 & \sin \alpha_1 & 0 \\ \sin \alpha_1 & \cos \alpha_1 & 0 \\ 0 & 0 & 1 \end{pmatrix} \begin{pmatrix} b \sin \alpha_1 \\ b \cos \alpha_1 \\ 0 \end{pmatrix} = \begin{pmatrix} 0 \\ b \\ 0 \end{pmatrix} = \vec{R}_1, \quad (19)$$

$$(ROT)\vec{R}_3 = \begin{pmatrix} -\cos \alpha_1 & \sin \alpha_1 & 0 \\ \sin \alpha_1 & \cos \alpha_1 & 0 \\ 0 & 0 & 1 \end{pmatrix} \begin{pmatrix} 0 \\ b \\ 0 \end{pmatrix} = \begin{pmatrix} b \sin \alpha_1 \\ b \cos \alpha_1 \\ 0 \end{pmatrix} = (ROT)\vec{R}_1, \quad (20)$$

and so on. Finally, we can find the following expressions for the terms with the rotation operators in Eq. (15),

$$\vec{R}_1 = (ROT)\vec{R}_2 = (ROT)\vec{R}_4 = \dots = \begin{pmatrix} 0 \\ b \\ 0 \end{pmatrix}, \quad (21)$$

$$\vec{R}_2 = (ROT)\vec{R}_1 = (ROT)\vec{R}_3 = (ROT)\vec{R}_5 = \dots = \begin{pmatrix} b \sin \alpha_1 \\ b \cos \alpha_1 \\ 0 \end{pmatrix}. \quad (22)$$

Substituting the relations above into the position equation Eq. (15), we get

$$\vec{P}_i = \vec{P}_1 + [(i-1)/2]\vec{R}_1 + [i/2]\vec{R}_2, \quad (23)$$

where  $[ ]$  denotes integer part, therefore, the configuration of the lipid chain is given as shown in Fig. 10a.



Now, another rotation operator ( $RT$ ) is used to rotate all the bond vectors of each chain by an angle  $\alpha_2 = 70.5^\circ/2$  around the  $Z$ -axis. The rotation operator is given by

$$(RT) = \begin{pmatrix} \cos \alpha_2 & \sin \alpha_2 & 0 \\ -\sin \alpha_2 & \cos \alpha_2 & 0 \\ 0 & 0 & 1 \end{pmatrix}. \quad (24)$$

As shown in Fig. 10b, the configuration of the chain after this operation is zigzagged along the  $Y$ -axis, perpendicular to the lipid bilayer plane. This is the initial rotational state of each chain, and is called the all-trans state.

### Interaction Energy Calculations

Before any Monte Carlo steps are done, the initial interaction energies must be calculated. There are three contributions to the interaction energies of a lipid chains. They are :

1. Each chain interacts with other chains via a 6-12 potential.
2. Each nearest neighbor chain of gramicidin A interacts with all non-hydrogen atoms on the gramicidin A monomer via a 6-12 potential.
3. Each residue of gramicidin A interacts with its nearest neighbor chains via a 6-12 potential.

The 6-12 potential used has the following form for an interaction between two molecules  $M_L$  and  $M_K$ , in which molecule  $M_L$  has a total of  $L$  atoms and molecule  $M_K$  has a total of  $K$  atoms :

$$E_{L,K} = \sum_{i=1}^L \sum_{j=1}^K \epsilon \left\{ \left( \frac{\sigma}{r_{i,j}} \right)^{12} - \left( \frac{\sigma}{r_{i,j}} \right)^6 \right\} + \frac{q_i q_j}{r_{i,j}}, \quad (25)$$

where  $r_{i,j}$  is the distance between atom  $i$  on molecule  $M_L$  and atom  $j$  on molecule  $M_K$ , and the sum runs over all atoms on both molecules. The interaction strength (*van der Waals* energy)  $\epsilon$  and *van der Waals* radius  $\sigma$  were calculated for hydrocarbon fluids by Jorgensen and co-workers [15] by optimizing the results of Monte

Carlo calculations relative to experimental data. Charges  $q_i$  and  $q_j$  are considered for polar molecules, when present (none are present in this research).

Because the quantity  $E_{L,K}$  decreases in magnitude rapidly with the increasing distance  $r_{i,j}$ , the calculation of  $E_{L,K}$  need only be carried out for chains within a certain cutoff radius of each other. The cutoff radius is set at 15 Å in all simulations.

In this research, the values chosen for the *van der Waals* parameters are

- For the interaction of CH<sub>2</sub> with CH<sub>2</sub>,  
 $\sigma = 3.983$  (Å) and  $\epsilon = 456.876$  (cal/mol);
- For the interaction of CH<sub>2</sub> with CH<sub>3</sub>,  
 $\sigma = 3.922$  (Å) and  $\epsilon = 475.343$  (cal/mol);
- For the interaction of CH<sub>2</sub> with O,  
 $\sigma = 3.906$  (Å) and  $\epsilon = 613.713$  (cal/mol);
- For the interaction of CH<sub>2</sub> with N,  
 $\sigma = 3.974$  (Å) and  $\epsilon = 459.857$  (cal/mol);
- For the interaction of CH<sub>2</sub> with C,  
 $\sigma = 3.984$  (Å) and  $\epsilon = 413.919$  (cal/mol);
- For the interaction of CH<sub>3</sub> with CH<sub>3</sub>,  
 $\sigma = 3.861$  (Å) and  $\epsilon = 724.528$  (cal/mol);
- For the interaction of CH<sub>3</sub> with O,  
 $\sigma = 3.845$  (Å) and  $\epsilon = 772.848$  (cal/mol);
- For the interaction of CH<sub>3</sub> with N,  
 $\sigma = 3.913$  (Å) and  $\epsilon = 579.097$  (cal/mol);
- For the interaction of CH<sub>3</sub> with C,  
 $\sigma = 3.922$  (Å) and  $\epsilon = 521.247$  (cal/mol).

### Procedure for Saving Old Configurations and Energies

Before running each Monte Carlo (MC) step, both the old configurations of gramicidin A and the lipid chains, including the position of atoms and their bond vectors, and the old interaction energies, are saved. During the MC procedure the old configuration energies must be compared with the new energies after a MC step to decide whether or not to accept the new configuration.

### Procedure for Picking a Chain

A chain is picked at random from the 94 available chains in the simulation cell.

### Procedure for Whole Chain Translation

The chosen chain is first translated in the  $X$ - $Z$  plane in a random direction by a random distance less than 0.15 Å. This is done simply by relocating the topmost carbon in the chains since successive carbons are generated from the top carbon by the rotation operations.

### Procedure for Gauche Rotations

At this point, a random number is called to determine whether or not gauche rotations should be performed on the chosen chain. If no gauche rotation is performed, the chain will be given a small random rotation around the molecular long-axis ( $Y$ -axis in this model), and will also randomly perform a lateral move as described above.

If one or more gauche rotations are to be performed on the chosen chain, then the procedure is as follows. First of all, one or two bonds on the chain are chosen randomly. Then the rotational state of the chosen bond is changed. In the rotational-isomeric approximation, the allowed angles for any gauche rotation are the dihedral angles  $0^\circ$ ,  $+120^\circ$ , and  $-120^\circ$ . Fig. 11a shows the relations of the three

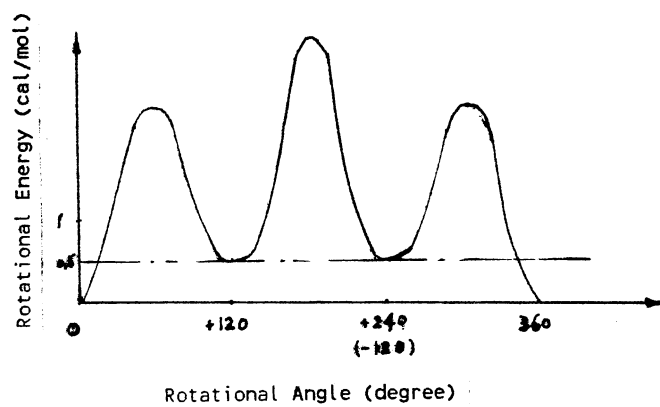
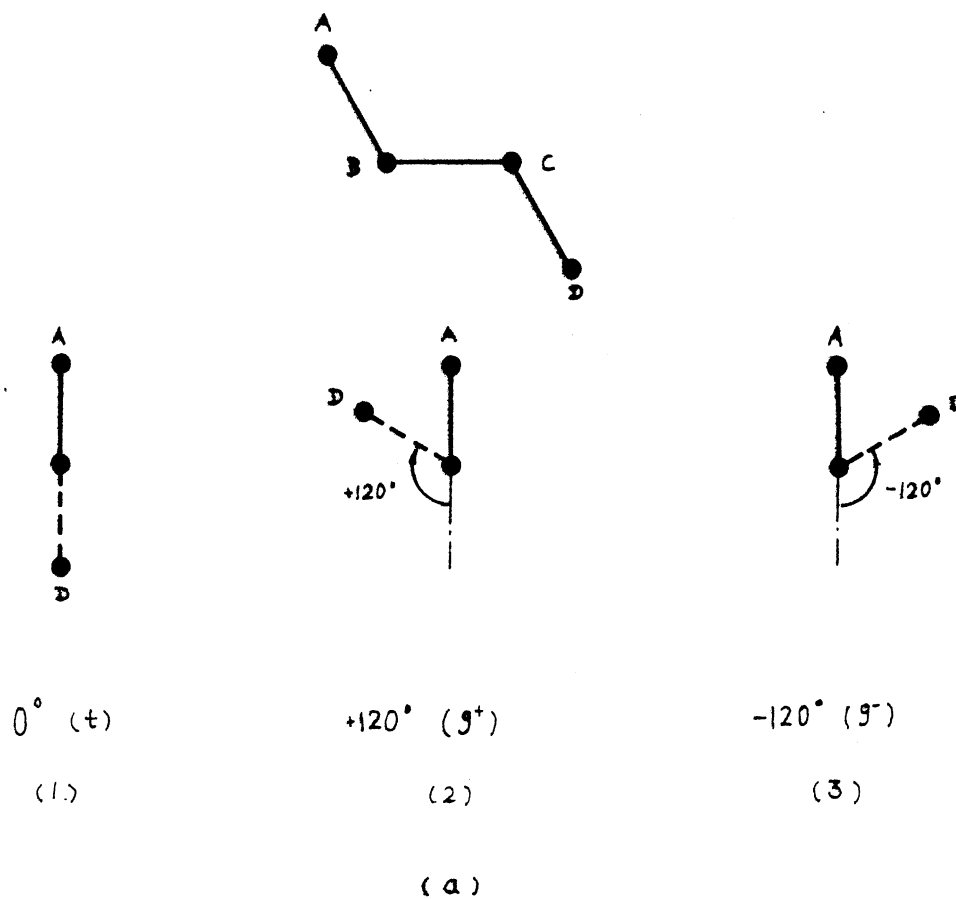


Figure 11. (a) Gauche rotations with (1) gauche angle zero; (2) gauche angle  $+120^\circ$ ; (3) gauche angle  $-120^\circ$  ( $+240^\circ$ ). (b) The potential energy as a function of rotation angle.

angles, and Fig. 11b shows a plot of the energies versus rotation angle, with the minima at  $0^\circ$  and  $\pm 120^\circ$ . For the gauche angle  $0^\circ$  (the trans state ( $t$ )) the energy is zero. Both the gauche angles  $\pm 120^\circ$ , ( $g^\pm$ ) have energy 500 (cal/mol). So, there are three possibilities for changes in gauche energies :

- Rotating from trans state ( $t$ ) to gauche states ( $g^\pm$ ), the chain gains energy 500 cal/mol;
- Rotating from gauche states ( $g^\pm$ ) to trans state ( $t$ ), the chain loses energy  $-500$  cal/mol.
- Rotating between gauche states ( $g^\pm$ ) and ( $g^\mp$ ), not any energy changes ( $+500 - 500 = 0$ ) for the chain take place.

One more case, that of successive gauche bonds, should be considered. These are strongly inhibited. If the nearest neighbor bonds of the chosen bonds are gauche states, when the chosen bonds are given gauche rotations either from trans state ( $t$ ) to gauche states ( $g^\pm$ ) or from gauche states ( $g^\pm$ ) to trans state ( $t$ ), the chain either gains or loses  $-2500$  (cal/mol) more energy due to each nearest neighbor bond's gauche state. This is because successive  $g^\pm g^\pm$  states are very unlikely due to steric overlap of neighboring  $\text{CH}_2$  molecules.

Now the procedure by which the chain coordinates are regenerated after a gauche rotation is performed will be described. Let the chosen bond be the  $k$ th bond of the chain as shown in Fig. 12a. If  $k$  is odd, the gauche rotation is performed by means of an operator  $RG$ :

$$(RG) = \begin{pmatrix} \cos \theta_N & 0 & \sin \theta_N \\ 0 & 1 & 0 \\ -\sin \theta_N & 0 & \cos \theta_N \end{pmatrix}, \quad (26)$$

where  $N = 1, 2, 3$  describes the gauche rotation angle.

$$\theta_1 = +120^\circ \quad (27)$$

$$\theta_2 = 0 \quad (28)$$

$$\theta_3 = -120^\circ \quad (29)$$

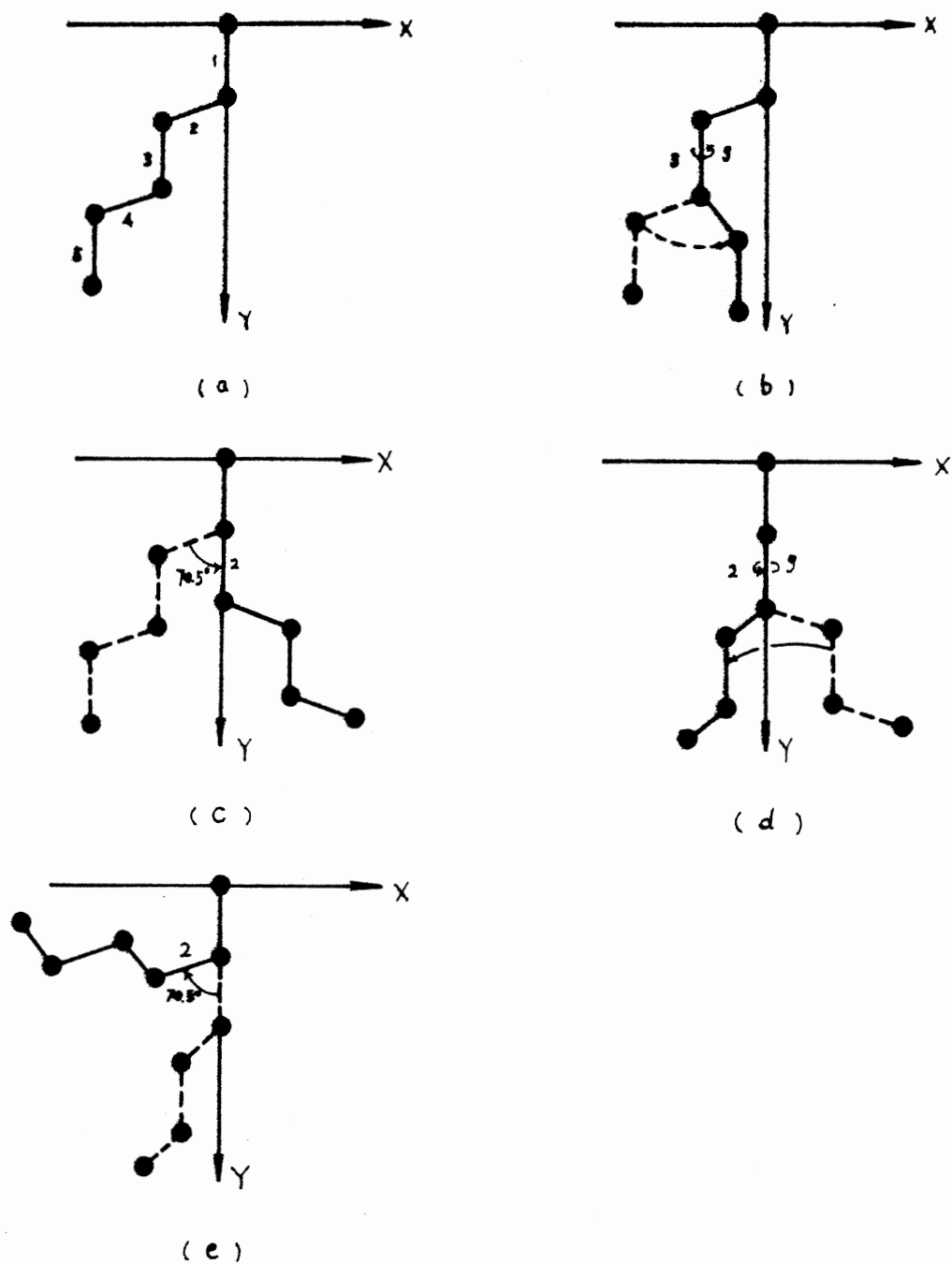


Figure 12. Procedure for gauche rotation for bond  $k$ : (a)  $\rightarrow$  (b) for  $k$  odd, the rotation operators are  $(ROT)$  and  $(GR)$ ; (a)  $\rightarrow$  (c)  $\rightarrow$  (d)  $\rightarrow$  (e) for  $k$  even, the rotation operators are  $(ROT)$ ,  $(ROTP)$ ,  $(GR)$  and  $(ROTP)^{-1}$ .

It must be pointed out that the changes in the position coordinates of the carbons on the chain occur only for the segments after bond  $k$  (not including bond  $k$ ). The positions of the changed segments can be given by

$$\vec{P}_{i+1} = \vec{P}_i + (RG)\vec{R}_i \quad (30)$$

where

$$(i = k, k + 1, k + 2, \dots, m - 1), \quad (31)$$

and  $m$  is the total number of carbons on the chain. The procedure of the gauche rotation for  $k$  being odd is shown in Fig. 12:  $a \rightarrow b$ .

If  $k$  is even, the segments starting with bond  $k$  (including bond  $k$ ) must be preceded by a rotation of  $\alpha_1$  ( $= 70.5^\circ$ ) around the  $Z$ -axis (see Fig. 12c) by means of an operator ( $ROTP$ )

$$(ROTP) = \begin{pmatrix} \cos \alpha_1 & \sin \alpha_1 & 0 \\ -\sin \alpha_1 & \cos \alpha_1 & 0 \\ 0 & 0 & 1 \end{pmatrix}. \quad (32)$$

Then the gauche rotations are performed by operator ( $RG$ ) and followed by a rotation of  $-\alpha_1$  using operator  $(ROTP)^{-1}$ . The procedure of gauche rotation for  $k$  even is shown pictorially in Fig. 12:  $a \rightarrow c \rightarrow d \rightarrow e$ .

#### Procedure for Long-Axis Rotation

Finally, the entire chain is rotated over a small angle  $\beta_y$  chosen at random, around the molecular long-axis by operator ( $ANG$ ). After this rotation the position coordinates of carbons are,

$$\vec{P}_{i+1} = \vec{P}_i + (ANG)\vec{R}_i \quad (33)$$

$$(i = 1, 2, 3, \dots, m - 1), \quad (34)$$

where

$$(ANG) = \begin{pmatrix} \cos \beta_y & 0 & \sin \beta_y \\ 0 & 1 & 0 \\ -\sin \beta_y & 0 & \cos \beta_y \end{pmatrix}. \quad (35)$$

## Periodic Boundary Conditions

After rotation and translation, some atoms of the chain may move out of the boundary of the simulation cell. To eliminate this problem periodic boundary conditions have been used in this project. That is, the atom which moved out from a boundary of the lipid chain array is considered to move into the array at the opposite boundary.

### Procedure for Change In Energy Calculations

After each Monte Carlo step, the new energy of the chain is calculated by means of the same procedure as that of the initial energy calculation. The energy differences  $\Delta E$  are given by

$$\Delta E_{total}(K) = \Delta E_{chain-chain}(K) + \Delta E_{chain-gramicidinA}(K) + \Delta E_{gauche}(K). \quad (36)$$

### Acceptance Criteria for Monte Carlo Moves

Accepting or rejecting a move depends upon the transition probability  $W_{\mu \rightarrow \mu'}$  (see *Chapter 2*), as a function of  $\Delta E_{total}(K)$ .

If the move is accepted then the configuration coordinates and energies are accordingly updated. If not, the values of these quantities are reset to the old values.

### Procedure for Gramicidin A Configuration Changes

The Monte Carlo procedure for a single lipid chain has been described above. Now the Monte Carlo method for gramicidin A will be considered. Because the residues of gramicidin A are much more mobile than the rigid  $\alpha$ -helical backbone, only the 15 residues of gramicidin A are allowed to change states. The following procedure is utilized: First, a bond on one of the 15 residues is picked at random. (For tryptophan residues, the allowed bonds for rotation are  $C^\alpha - C^\beta$  and  $C^\beta - C^\gamma$  due to the aromatic structure.) Let  $\vec{r}_k$  be the bond vector of the chosen



bond, and  $l, m, n$  be the projections of  $\vec{r}_k$  in the directions of  $X, Y$  and  $Z$  axis (see Fig13a). The angles between the bond and the  $X, Y$  and  $Z$  axes are, respectively,

$$\beta_1 = \arccos^{-1}\left(\frac{l}{|\vec{r}_k|}\right), \quad (37)$$

$$\beta_2 = \arccos^{-1}\left(\frac{m}{|\vec{r}_k|}\right), \quad (38)$$

$$\beta_3 = \arccos^{-1}\left(\frac{n}{|\vec{r}_k|}\right). \quad (39)$$

Let  $\alpha_1, \alpha_2$  and  $\alpha_3$  be the angles between the chosen bond vector  $\vec{r}_k$  and the  $Y - Z$ ,  $Z - X$ , and  $X - Y$  planes, respectively,

$$\alpha_1 = \pi/2 - \beta_1, \quad (40)$$

$$\alpha_2 = \pi/2 - \beta_2, \quad (41)$$

$$\alpha_3 = \pi/2 - \beta_3. \quad (42)$$

Let  $C'$  be the angle between the projection of  $\vec{r}_k$  on the  $Y - Z$  plane and the  $X - Y$  plane, and let  $A$  be the angle between  $\vec{r}_k$  and its projection on the  $Y - Z$  plane (see Fig. 13b). From Fig. 13c, the relation of the angle  $C'$  with  $\beta$  is given by:

$$r_{23} = r \cos \alpha_1 = r \cos(\pi/2 - \beta_1) = r \sin \beta_1, \quad (43)$$

$$l = r \sin \alpha_3 = r \sin(\pi/2 - \beta_3) = r \cos \beta_3, \quad (44)$$

$$l' = l, \quad (45)$$

$$\sin C' = \frac{l'}{r_{23}} = \frac{\cos \beta_3}{\sin \beta_1}. \quad (46)$$

The vector  $\vec{r}_k$  may exist in any octant of the Cartesian coordinate system. Therefore eight situations must be considered corresponding to the eight octants in the Cartesian system. The resulting expressions for the angles  $A$  and  $C$  are shown in Fig. 14, where  $C$  is the angle between the projection of  $\vec{r}_k$  on the  $Y - Z$  plane and the  $Y$  axis. These angles are needed to calculate the coordinates of the residues after a rotation about the chosen bond is made. The side chains of the gramicidins in a biomembrane execute rapid fluctuations of small angular amplitude [23]. Let  $\theta$  be a very small random angle. The side chain rotation procedure consists of three steps including five rotation operations :

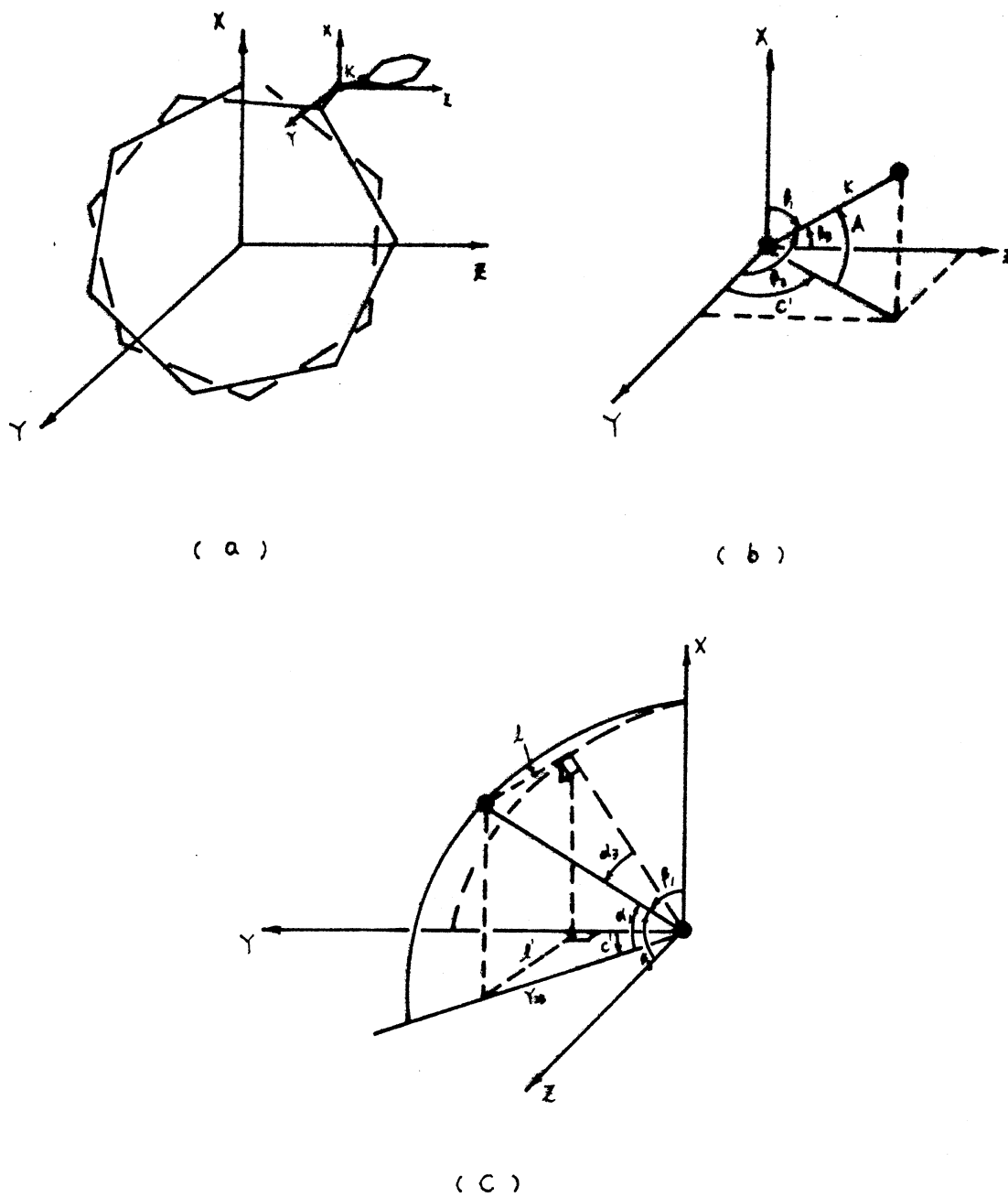


Figure 13. Pictorial description of the chosen bond  $k$  on a residue of gramicidin A: (a) location of the bond and the coordinate axes; (b) the relations of angle  $A$  with angle  $C'$ ; (c) the pictorial description for the derivation of  $\sin C'$ .

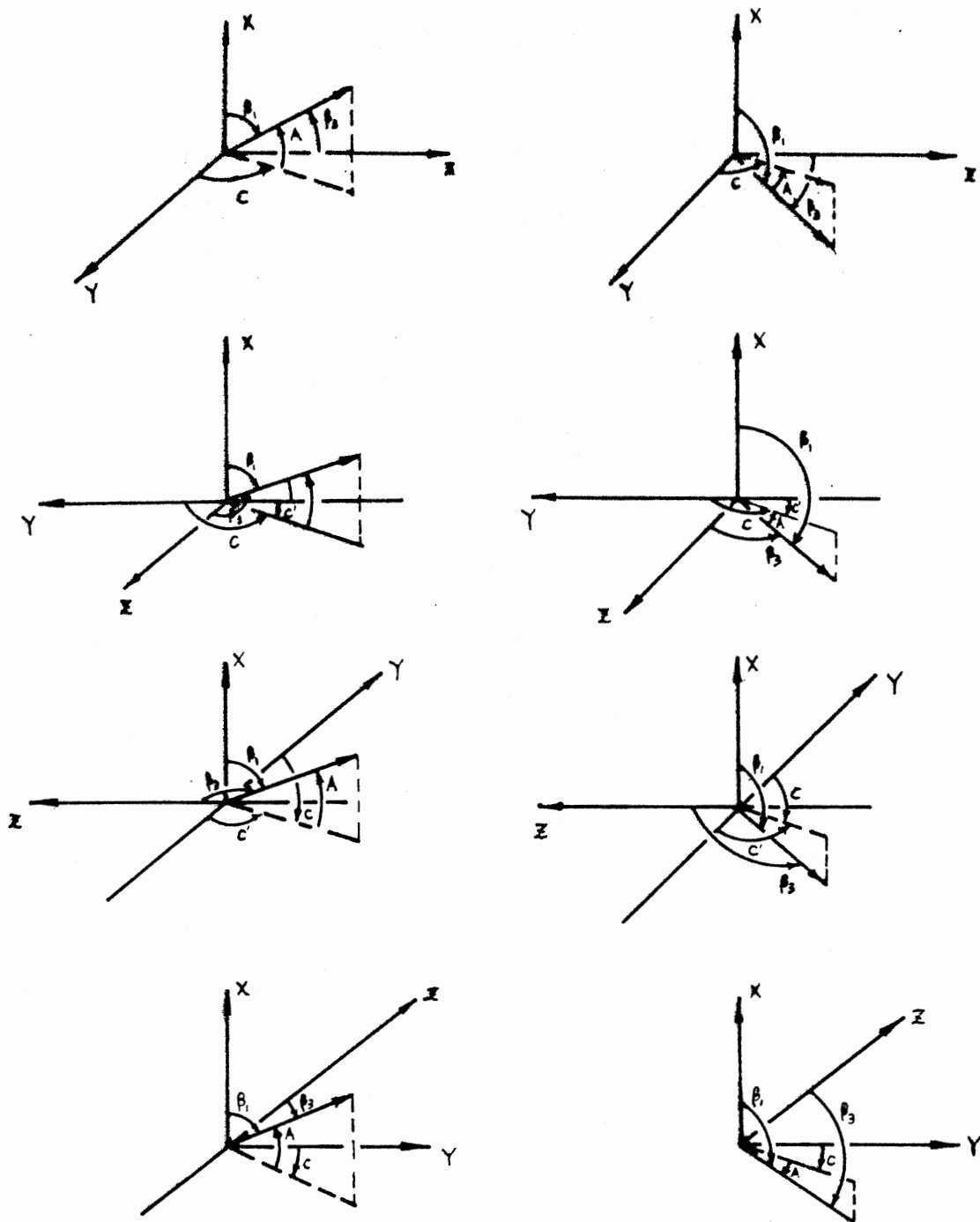


Figure 14. The relations of angle  $A$  with angle  $C$  corresponding to the eight octants in the Cartesian system.

- Rotate the chosen bond to the  $Y$ -axis ( either  $X$ - or  $Z$ - axes could also be chosen) by first performing two rotation operations  $(R_x^a)$  and  $(R_z^a)$ ,

$$(R_x^a) = \begin{pmatrix} 1 & 0 & 0 \\ 0 & \cos C & \sin C \\ 0 & -\sin C & \cos C \end{pmatrix} \quad (47)$$

and

$$(R_z^a) = \begin{pmatrix} \cos A & -\sin A & 0 \\ \sin A & \cos A & 0 \\ 0 & 0 & 1 \end{pmatrix}. \quad (48)$$

The bond vectors after these rotation are

$$\vec{r}_j^a = (R_z^a)(R_x^a)\vec{r}_j^i, \quad (49)$$

$$(j = k, k + 1, k + 2, \dots, N_L), \quad (50)$$

where  $\vec{r}_j^i$  belongs to the  $L$ th residue,  $k$  is the picked bond on this residue,  $N_L$  is the largest number of the  $L$ th residue.

- Now rotate the chosen bond by the random angle  $\theta$  about the  $Y$ -axis,

$$(R_y^\theta) = \begin{pmatrix} \cos \theta & 0 & -\sin \theta \\ 0 & 1 & 0 \\ \sin \theta & 0 & \cos \theta \end{pmatrix}. \quad (51)$$

After this rotation, the bond vectors after the  $k$ th bond is

$$\vec{r}_j^\theta = (R_y^\theta)\vec{r}_j^a, \quad (52)$$

$$(j = k + 1, k + 2, k + 3, \dots, N_L). \quad (53)$$

- Rotate back to the original coordinate system using rotation operators  $(R_z^a)^{-1}$  and  $(R_x^a)^{-1}$ .

The entire procedure is finished after these rotations. The new bond vectors are given by

$$\vec{r}_j^i = (R_x^a)^{-1}(R_z^a)^{-1}\vec{r}_j^\theta. \quad (54)$$

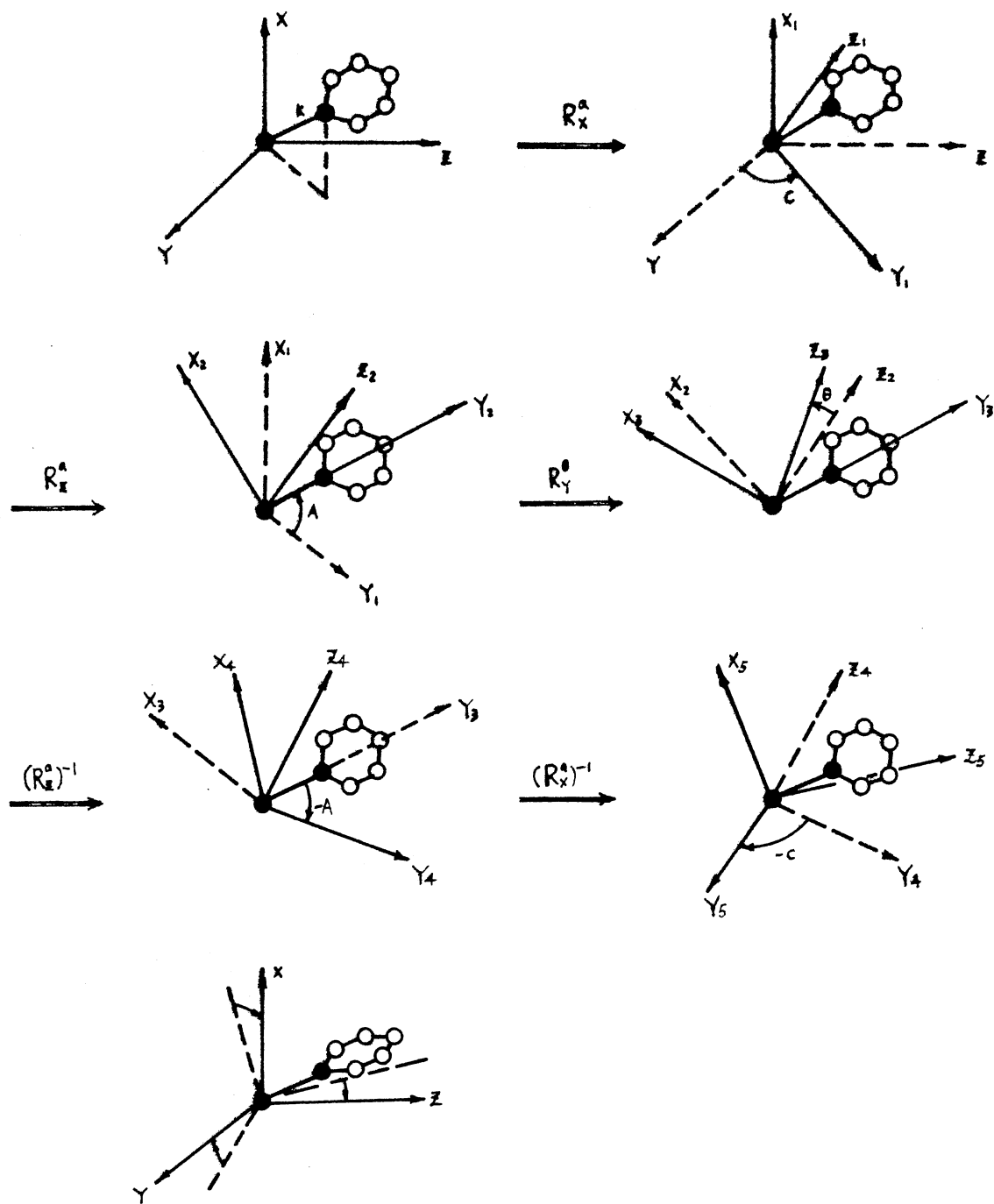


Figure 15. Pictorial procedure of the rotations around the chosen bond  $k$  on a residue of gramicidin A with rotation operators  $(R_x^\alpha)$ ,  $(R_z^\alpha)$ ,  $(R_y^\theta)$ ,  $(R_z^\alpha)^{-1}$  and  $(R_x^\alpha)^{-1}$ .

Fig. 15 shows the entire procedure described above. The new residue energy is calculated by Eq. (25), and the same Monte Carlo algorithm for accepting or rejecting the move is used.

### Procedure for Calculating Averages

In Chapter 2, we have shown that in a Monte Carlo simulation any observable quantity can be calculated as an arithmetic average, see Eq. (5),

$$\langle A \rangle = \frac{1}{M} \sum_{\mu=1}^M A(\mu). \quad (55)$$

In this research, the observable quantity which has been chosen is the segmental order-parameter profile

$$S_n = \frac{1}{2} \langle 3 \cos^2 \theta_n - 1 \rangle \quad (56)$$

where  $\theta_n$  is the deviation of the  $n$ th bond from its orientation in the trans conformation. The orientation of the  $n$ th bond has an angle  $\theta_n^\circ$  between the bond and the  $Z - X$  plane in the trans conformation.

$$\theta_n = \theta'_n - \theta_n^\circ \quad (57)$$

where  $\theta_n^\circ = 54.75^\circ$  and  $\theta'_n$  is the angle after the bond moved (see Fig. 16). Three sets of order-parameter profiles have been calculated :

- For all chains except the twelve nearest neighbor chains of gramicidin A,

$$S_n = \frac{\sum^{mcs} \sum^{chains-12} (1/2)(3 \cos^2 \theta_n - 1)}{M_{mcs}(chains - 12)} \quad (58)$$

where  $mcs$  means the number of Monte Carlo steps, and  $M_{mcs}$  is the total number of configurations of system for the Monte Carlo run.

- For the twelve nearest neighbor chains of gramicidin A,

$$S_n = \frac{\sum^{mcs} \sum^{12} (1/2)(3 \cos^2 \theta_n - 1)}{M_{mcs}(12)} \quad (59)$$

- For the eighteen next-nearest neighbor chains of gramicidin A,

$$S_n = \frac{\sum^{mcs} \sum^{18} (1/2)(3 \cos^2 \theta_n - 1)}{M_{mcs}(18)} \quad (60)$$

The results of the calculations will be discussed in *Chapter 4*.

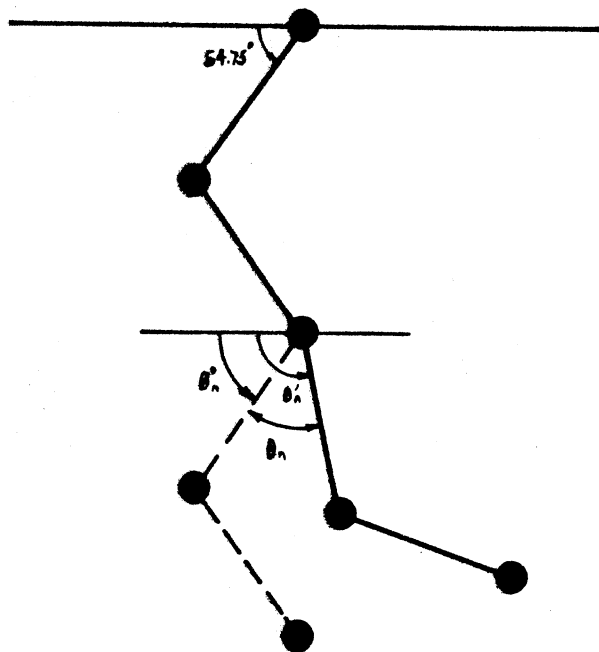


Figure 16. The relations between bond angles  $\theta_n^\circ$ ,  $\theta'_n$  and  $\theta_n$ :  
 $\theta_n^\circ$  is the original angle;  $\theta'_n$  is the new angle;  
 $\theta_n$  is the deviation.

### 3-2 Run Procedures

The computer program for this research was written in FORTRAN and much of the code has been vectorized. Most of the calculations were performed on the Cray X-MP/48 at the National Center for Supercomputing Applications. The basic procedure used in running the program were :

1. The lipid-gramicidin system was initially started with all chains in all-trans configurations. The Monte Carlo algorithm was run for 3 million configurations to equilibrate the system.
2. Another 3 million configurations were generated for the calculation of the order parameters.

Both the DMPC and the DPPC runs were carried out at 300 °K. The errors for both systems are estimated as standard deviations in the average of the calculations for every 2500 passes.



## CHAPTER IV

### RESULTS & DISCUSSION

#### 4-1 Results

In this chapter the results of the simulations, which consist of plots of order-parameter profiles, graphic pictures of typical configurations and standard deviations for both systems, will be described. They will also be compared with experimental data from  $^2\text{H-NMR}$ .

#### DMPC-Gramicidin A System

Fig. 17 is a plot of the order-parameter profiles for the nearest neighbors of gramicidin A and for all other chains. It is clear that the two sets of profiles are different due to the effect of gramicidin A. In the region of upper bonds, from bonds 1–5, the gramicidin neighbor chains have the almost identical order as do the bulk chains. The length of this region is about  $6.25 \text{ \AA}$  ( $1.25 \text{ \AA} \times 5 = 6.25 \text{ \AA}$ , see Fig. 18) which is approximately equal to the thickness of the region from the residues 15–7 on gramicidin A ( $6.27 \text{ \AA}$ ). This is the part of gramicidin A, which includes four tryptophans and two leucines ( see Appendix A). The partial ordering of the upper region of gramicidin-neighbor chains is likely due to the fact that the larger residues have a very large excluded volume, leaving little room for the chains to show rotational disorder.

After the 5th bond, the value of the order parameter for gramicidin neighboring chains is lower than that of bulk chains. This situation is also a result of the presence of the gramicidin A monomer. As shown in Fig. 18a, the volume occupied by gramicidin A from residues 7 through the terminal formyl group is

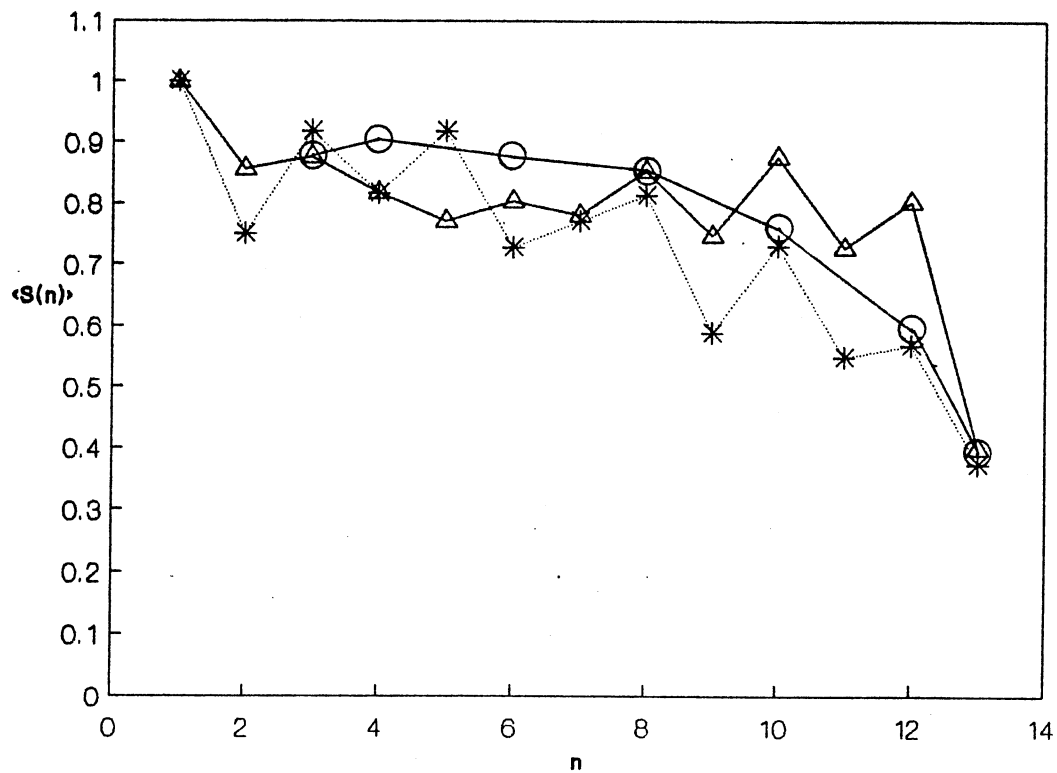


Figure 17. Order-parameter profile  $\langle S_n \rangle$  vs bond number  $n$  for calculated averages from DMPC (C-14) simulations: ( $\Delta$ ) average for all chains; (\*) average for nearest-neighbor chains of gramicidin A; ( $\circ$ ) experimental data from  $^2\text{H-NMR}$ .

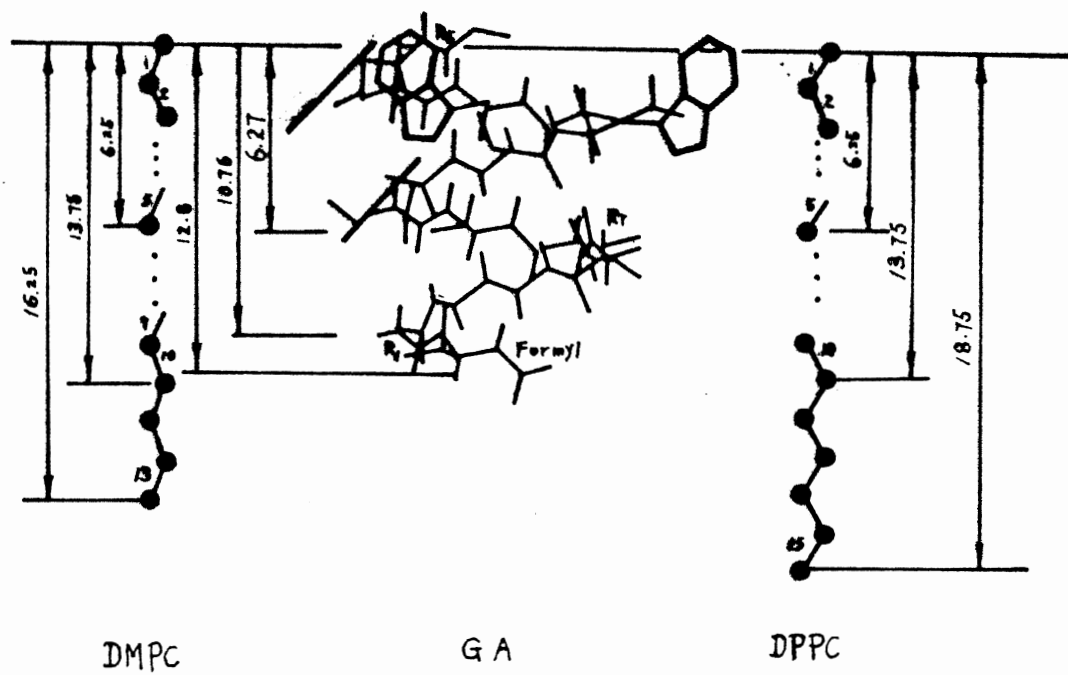


Figure 18. Size comparison of gramicidin A with DMPC and DPPC chains.

smaller than that occupied by the residues in the upper part of the polypeptide. The neighboring chains, therefore, have more volume available compared to the bulk chains.

From the 9th bond to the end of chain, the plot of the order-parameter profile for the gramicidin-neighboring chains decreases markedly, presenting distinct disorder. The reason is clearly due to the total height of gramicidin A being only about 12.8 Å (see Fig. 18). The bonds on the chains which extend beyond this length can, therefore, move freely into the space under the gramicidin A monomer. The experimental order-parameter profile for pure DMPC chains are given by the quadrupole splitting data of  $^2\text{H-NMR}$  [33]. Appendix B gives a procedure of calculating the experimental order parameters from the quadrupole splitting data. Fig. 19 shows the top view and side view of a typical configuration of gramicidin A and its neighboring chains after 60,000 MC steps. From the side view, it is quite clear that in the region above the 5th bond the chains partially remain in trans states, but, after the 5th bond, configurations consist of mixed trans, kink and jog states. Table I gives the standard deviations for DMPC-GA system.

### DPPC-Gramicidin A System

DPPC chains, which have 15 carbon-carbon bonds, are two carbons larger than DMPC chains (see Fig.18b). The results of the order-parameter profile  $\langle S_n \rangle$  calculations for the DPPC-gramicidin A system are shown in Fig. 20. As in the DMPC simulations, the order-parameter profile  $\langle S_n \rangle$  for the neighboring chains is very close to that for bulk chains above the 5th bond. This result implies that the steric hindrance effect of gramicidin A on lipid chains is not noticeable, so that the behavior of neighboring chains is similar to the bulk chains above the 5th bond. From bonds 5-10, the order-parameter profile for the neighboring chains is also almost the same as bulk chains. However, it decreases sharply at bond 10. From bond 11 to the end of chain, the order-parameter profile for the neighboring chains is lower than but close to the bulk chains. Bond 10 is located at the bottom of the gramicidin A monomer, so for neighboring chains of gramicidin A, it is quite

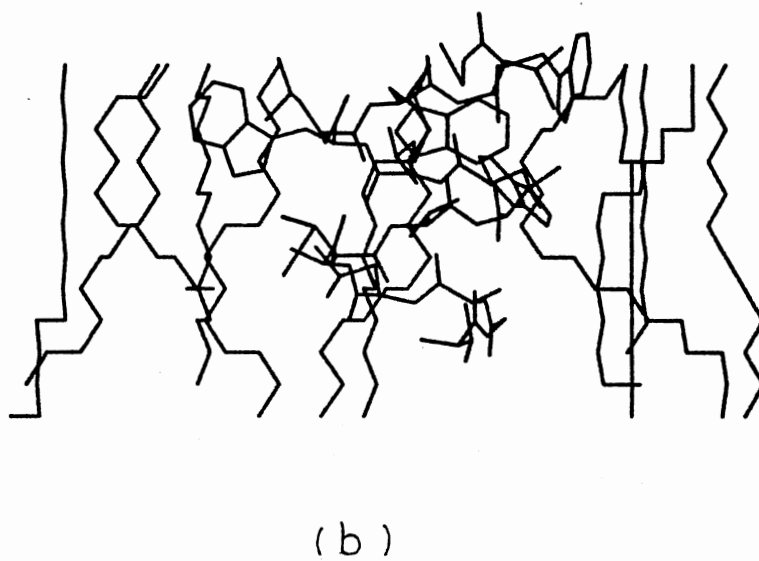
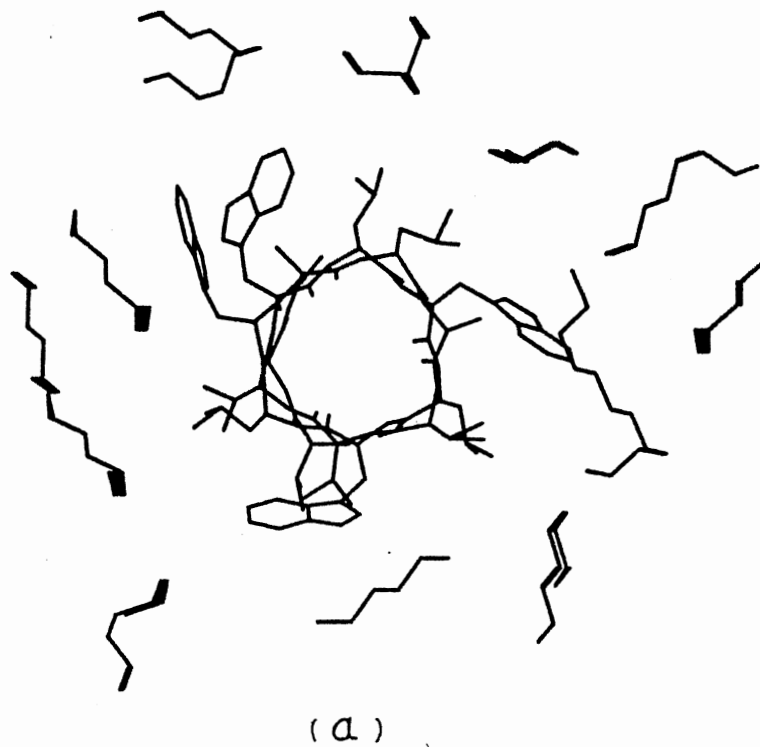


Figure 19. Top view and side view of a typical configuration of gramicidin A and its neighbor chains (DMPC) after 60,000 MC steps, (a) top view; (b) side view.

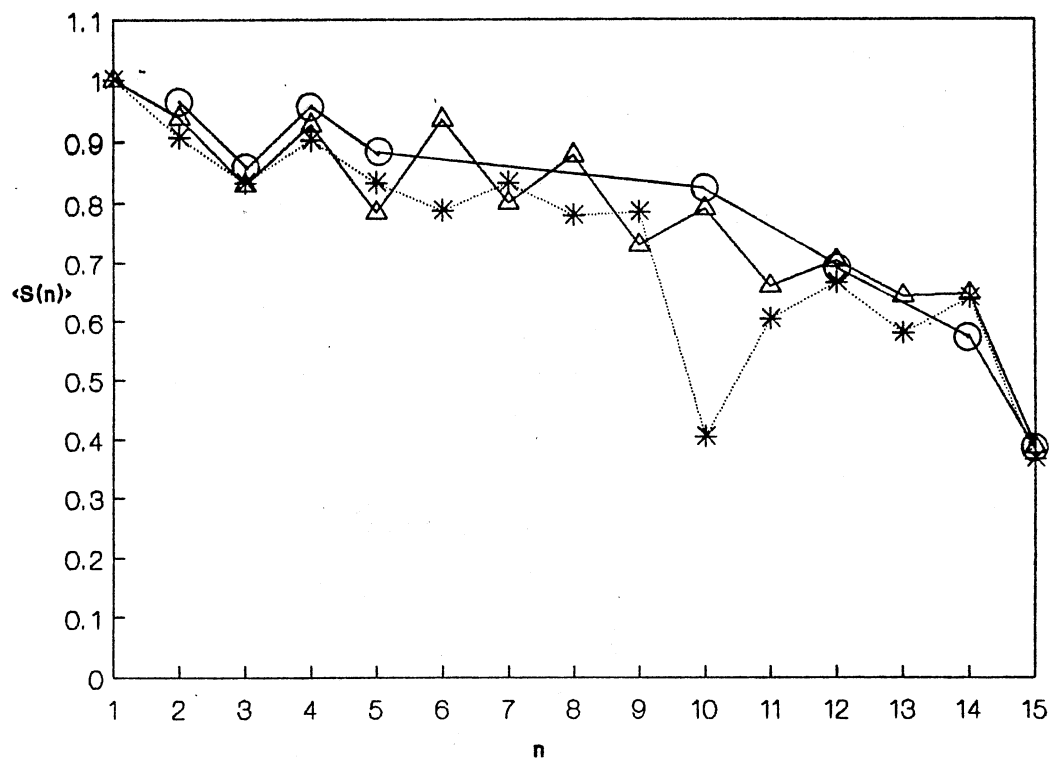


Figure 20. Order-parameter profile  $\langle S_n \rangle$  vs bond number  $n$  for calculated averages from DPPC (C-16) simulations: ( $\Delta$ ) average for all chains; (\*) average for nearest-neighbor chains of gramicidin A; (o) experimental data from  $^2\text{H-NMR}$ .

different from other bonds. That the segments of bonds 11-15 are a little more disordered than the bulk chains is likely due to the fact that the short height of gramicidin A gives the 10th bond a good chance to move. On the other hand, however, segments 11-15 are of such sufficient length that they can not easily move into the small cylindric region whose diameter is only 4 Å. Therefore, what is likely is that bond 10 is the middle bond on the highest kink-like conformations that can occur with ease. Similar experimental data was reported by Seelig and co-workers [42].

Fig. 21 shows the top view and side view for the DPPC-gramicidin A system. The picture is quite clear: the upper region (carbon bonds 1-5) for neighboring chains of gramicidin A tends to remain in partial trans states; at the region about bond 10, a distinct change in configuration is seen due to the termination of the gramicidin A monomer. The standard deviations for DPPC-GA system are shown in table II.

#### 4-2 Discussion

In summary, a gramicidin A monomer has been taken as a model of the membrane protein spanning membrane bilayers of two different lipid chains, DMPC (C-14) and DPPC (C-16). For the lipid chains-gramicidin A system in this research, the common conclusions from the results mentioned above and some discussion are given in turn :

1. The four tryptophan rings of gramicidin A, being consequently situated toward the polar surfaces of the membrane rather than its interior [23], are exposed to the upper region of the hydrophobic environment of the lipid fatty acyl chains. This construction results in a cone shape whose effect on chain ordering is very slightly greater for bonds in the middle or lower parts of the chains.
2. The two kinds of chains, DMPC and DPPC, have some differences in their lipid-gramicidin A monomer interactions. In the upper region of the chains

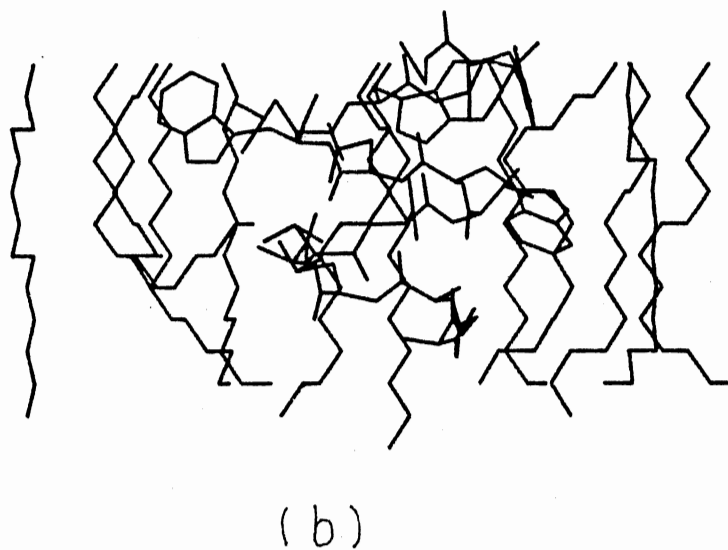
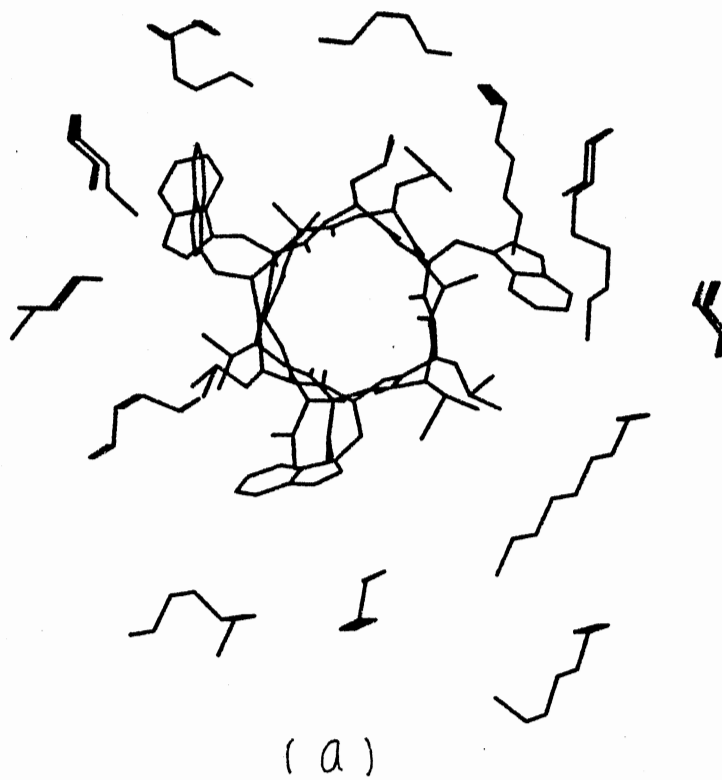


Figure 21. Top view and side view of a typical configurations of gramicidin A and its neighbor chains (DPPC) after 60,000 MC steps, (a) top view; (b) side view.



(before the 10th bond), the ordering behavior for both of them is almost the same as that of bulk chains though the DMPC chain is partially ordered before the 5th bond and partially disordered in the region near bonds 5-9. After the 10th bond, both DMPC and DPPC are slightly more disordered than bulk chains.

3. From the results, we can speculate about the case of a gramicidin A dimer in a model membrane bilayer, consisting of an N-terminal to N-terminal helical channel ( see Fig. 7). The neighboring chains of the dimer may not be different from bulk chains due to the fact that no free space under the gramicidin A monomer does exist.
4. There are 47 lipid molecules (94 chains) and one gramicidin A molecule in this study, so the concentrations of gramicidin A for both DMPC and DPPC system are given as follows: for DMPC, the weight percentage of gramicidin A is  $wt \% \approx 5.78 \%$  or lipid : gramicidin A  $\approx 47 : 1$ ; for DPPC,  $wt \% \approx 5.35 \%$  or lipid : gramicidin A  $\approx 47 : 1$ . Those concentrations are so low that the effect of gramicidin A monomer on lipid chains is confined to near neighbor chains only. For this reason, the equilibrium properties of the gramicidin neighbor chains in this study are almost the same as those of the bulk chains. Fig. 22 shows experimental data of deuterium quadrupole splitting (a) for the last carbon of DMPC versus weight percentage of gramicidin or moles of lipid : moles of gramicidin and (b) for DMPC chains versus carbon numbers [33]. We have translated the deuterium quadrupole splitting data to the order-parameter profile  $S_n$  by means of the procedure in Appendix B. (a') shows the result of  $S_n$  corresponding to (a). In (a'), the order parameter for  $wt \% = 5 \%$  is close to that of pure chains ( $wt \% = 0$ ). From Figs. 17, 20 and 22a', We can conclude that our results basically agree with the experimental data. In future work, we may simulate various ratios of lipid : gramicidin and compare the results with experimental data.

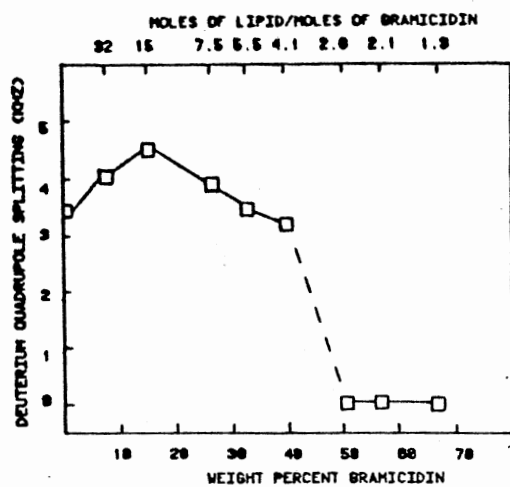


FIGURE 2: A plot of deuterium quadrupole splitting for 2-[14',14'- $^2\text{H}_2$ ]DMPC vs. weight percent gramicidin A'. The top horizontal axis shows moles of lipid per mole of gramicidin. Data were recorded at 30 °C. The broken line indicates a region in which two-component (powder pattern plus isotropic peak) spectra are observed.

(a)

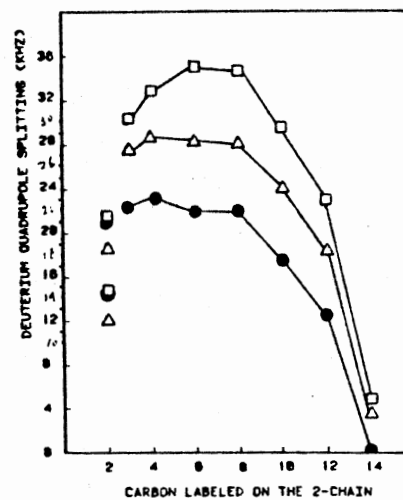
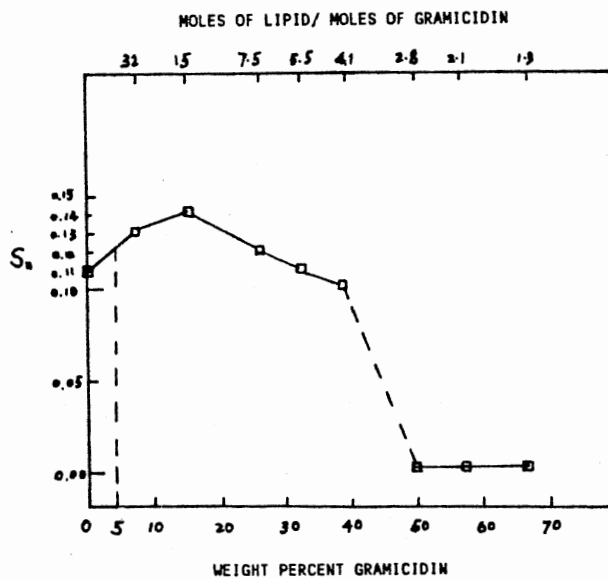


FIGURE 6: A plot of deuterium quadrupole splitting in kilohertz for DMPC vs. deuterium position on the 2-chain. The splittings were derived from the best theoretical fit by using a single splitting and Lorentzian line broadening. ( $\Delta$ ) Pure lipid; ( $\square$ ) 15 wt % gramicidin; ( $\bullet$ ) 50 wt % gramicidin. Sample temperature was 30 °C.

(b)



(a')

Figure 22. Experimental data from  $^2\text{H}$ -NMR; (a') shows the order parameter profile  $S_n$  corresponding to (a). Taken from Rice and Oldfield [33].

5. In Tables I and II we give the standard deviations for the calculations. These were obtained from analysis of fluctuations in the data during a single production run. Estimates of errors which would result from multiple run statistics are  $\pm 0.05$  for  $n \leq 5$ , and  $\pm 0.10$  for  $6 \leq n \leq 14$  or  $16$  where  $n$  is the bond number. Standard deviations for the chains which are neighbors of the gramicidin A may be compared to standard deviations of the bulk chains to estimate the extent to which the gramicidin A hinders conformational changes in its neighbor chains (as in [39]). It is clear that there is same hindrance in the upper portions of the chains, but this effect is not nearly so pronounced as the effect of cholesterol on its neighbor chains [39]. This is likely due to the roughness of the gramicidin A-lipid interface (at a molecular level), which contrasts with the relatively smooth rigid planar sterol rings in cholesterol.

Although the lipid-gramicidin A system is an oversimplified model of most biologically interesting membrane channels and pumps, the study of these model systems provides the basis on which we may begin to gain a better understanding of these systems in biological membranes.

TABLE I  
STANDARD DEVIATIONS OF  
<  $S_n$  > FOR DMPC DATA

bond no.	bulk chains	GA neighbor chains
2	0.013	0.003
3	0.001	0.014
4	0.011	0.005
5	0.012	0.023
6	0.022	0.024
7	0.005	0.031
8	0.021	0.049
9	0.024	0.029
10	0.014	0.050
11	0.006	0.053
12	0.035	0.056
13	0.031	0.034

TABLE II  
STANDARD DEVIATIONS OF  
<  $S_n$  > FOR DPPC DATA

bond no.	bulk chains	GA neighbor chains
2	0.004	0.002
3	0.014	0.000
4	0.004	0.040
5	0.019	0.000
6	0.008	0.018
7	0.014	0.000
8	0.005	0.008
9	0.014	0.065
10	0.007	0.081
11	0.010	0.029
12	0.027	0.026
13	0.020	0.039
14	0.030	0.022
15	0.073	0.053

## BIBLIOGRAPHY

1. Andersen, O. S., Koeppe, R. E., Durkin, J. T., and Mazit, J. L., *Ion Transport Through Membranes*, Academic press, New York, (1987).
2. Andersen, O. S., *Annu. Rev. Physiol.*, 46, 531-548, (1984).
3. Arseniev, A. V., Bystrov, V. F., Ivanov, V. T., and Ovchinnikov, Y. A., *FEBS Lett.*, 165, 51-56, (1984).
4. Arseniev, A. S., Barsakev, I. L., Bystrov, V. F., Lomize A. L., and Ovchinnikov, Y. A., *FEBS Lett.*, 186, 168-174, (1985).
5. Barrett Russell, E. W., Weiss, L. B., Navetta, F. I., and Koeppe, R. E., *Biophys. J.*, 49, 673-686, (1986).
6. Bamberg, E., and Janko, K., *Biochim. Biophys. Acta*, 465, 486-499, (1977).
7. Binder, K.,(Ed.): *Monte Carlo Method in Statistical Physics*, Springer-Verlag, New York, (1979).
8. Boni, L. T., Connolly, A. J., and Kleinfeld, A. M., *Biophys. J.*, 49, 122-123, (1986).
9. Burnett, L., and Muller, B. H., *J. Chem. Phys.*, 55, 5829, (1971).
10. Etchebest, C., and Pullman, A., *J. Biomol. Struct. Dyn.*, 2, 859, (1985).
11. Higgs, T. P., and McKay, A. L., *Chem. Phys. Lipids*, 20, 105, (1977).
12. Hesketh, T. R., Smith, G. A., Houslay, M. D., McGill, K. A., Birdsall, N. J. M., Metcalfe, J. C., and Warren, G. B., *Biochemistry*, 15, 4145, (1976).
13. Hotchkiss, R. D., *J. Biol. Chem.*, 141, 155, (1941).
14. Hussin, A., and Scott, H. L., *Biochim. Biophys. Acta*, 897, 423, (1987).
15. Jorgensen, *J. Chem. Phys.*, 77, 4156, (1982).
16. Jost, P., Griffith, O. H., Capaldi, R. A., and Vanderkooi, G., *Proc. Natl. Acad. Sci. USA.*, 70, 480, (1973).
17. Jost, P., and Griffith, O. H., in *Cellular Function and Molecular Structure. A Symposium on Biophysical Approaches to Biological Problems*, (Agris, P. F., Loepky, R. N., and Sykes, B. D., Eds.), p. 25.

18. Kim, K. S., and Clementi, E., *J. Amer. Chem. Soc.*, 107, 5504-5513, (1985).
19. Koeppe, R. E., and Schoenborn, B. P., *Biophys. J.*, 45, 503-507, (1984).
20. Kolb, H. -A., and Bamberg, E., *Biochim. Biophys. Acta*, 464, 127-141, (1977).
21. Lee, D. C., Durrani, A. A., and Chapman, D., *Biochim. Biophys. Acta*, 769, 49-56, (1984).
22. Luzzati, V., *Biological Membranes* (ed. D. Chapman), pp. 71-123. New York, N. Y. Academic Press, (1968).
23. Macdonald, P. M., and Seelig, J., *Biochim.* 27, 2357-2364, (1988).
24. Metropolis, N., Rosenbluth, A. W., Rosenbluth, M. N., Teller, A. H., and Teller, E., *J. Chem. Phys.*, 21, 1087, (1953).
25. Morrow, M. R., and Davis, J. H., *Biochim.* 27, 2024-2032, (1988).
26. Müller-Krumbhaar, H., and Binder, K., *J. Statist. Phys.*, 8, 1, (1973).
27. Nagle, J. F., and Scott, H. L., *Physics Today*, 31(Feb.), p. 38-47, (1978).
28. Naik, V. M., and Krimm, S., *Biophys. J.*, 49, 1131-1145, (1986).
29. Naik, V. M., and Krimm, S., *Biophys. J.*, 49, 1147-1154, (1986).
30. Neher, E., and Eibl, H. -J., *Biochim. Biophys. Acta*, 464, 37-44, (1977).
31. Prasad, K. U., Alonso-Romanowski, S., Venkatachalam, C. M., Trapane, T. L., and Urry, D. W., *Biochemistry*, 25, 456-463, (1986).
32. Ramachandran, G. N., and Chandrasekaran, R., *Indian J. of Biochim. and Biophys.*, 9, 1-11, (1971).
33. Rice, D., and Oldfield, E., *Biochemistry*, 18, 3272-3279, (1979).
34. Reinhard, S., and Witkop, B., *J. Amer. Chem. Soc.* 87, 2011, (1965).
35. Schreier, S., Polnaszek, C. F., and Smith, I. C. P., *Biochim. Biophys. Acta*, 515, 375, (1978).
36. Scott, H. L., *Biochim. Biophys. Acta*, 469, 264, (1977).
37. Scott, H. L., and Cherng, S.-L., *Biochim. Biophys. Acta*, 510, 209, (1978).
38. Scott, H. L., *Biochemistry*, 25, 6122, (1986).
39. Scott, H. L., and Kalaskar, S., *Biochemistry*, 28, 3687, (1989).

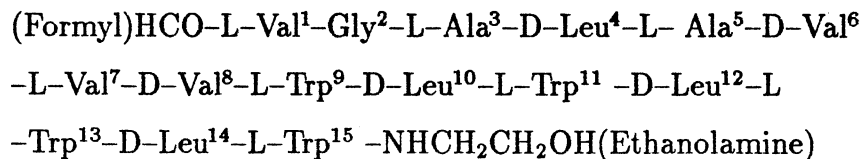
40. Scott, H. L., in *Molecular Description of Biological Membrane Components by Computer Aided Conformational Analysis*, (R. Brasseur, Ed.), CRC Press, 1989.
41. Seelig, J., and Niederberger, W., *J. Amer. Chem. Soc.*, 96, 2069, (1974).
42. Seelig, A., and Seelig, J., *Biochemistry N. Y.*, 13, 4839-4845, (1974).
43. Seelig, A., and Seelig, J., *Biochim. Biophys. Acta*, 406, 1-5, (1975)
44. Seelig, A., and Seelig, J., *Biochemistry N. Y.*, 16, 45-50, (1977).
45. Seelig, J., Gally, H. U., and Wohlgemuth, R., *Biochim. Biophys. Acta*, 467, 109-119, (1977).
46. Seelig, J., and Seelig, A., *Rev. Biophys.*, 13, 19, (1980).
47. Urry, D. W., Goodall, M. C., Lickson, J. D. G., and Mayers, D. F., *Proc. Nat. Acad. Sci. USA*, 68, 8, 1907-1911, (1971).
48. Urry, D. W., in *The Enzymes of Biological Membranes*, (Martonosi, A. N., Ed.), 1, 229-257, Plenum, N.Y., (1985).
49. Veatch, W., and Stryer, L., *J. Mol. Biol.*, 113, 89-102, (1977),
50. Wallace, B. A., *Biophys. J.*, 49, 295-306, (1986).
51. Weinstein, S., Wallace, B. A., Blout, E. R., Morrow, J. S., and Veatch, W., *Proc. Natl. Acad. Sci. USA*. 76,4230-4234, (1979).
52. Weinstein, S., Wallace, B. A., Morrow, J. S., and Veatch, W. R., *J. Mol. Biol.*, 143, 1-19, (1980).



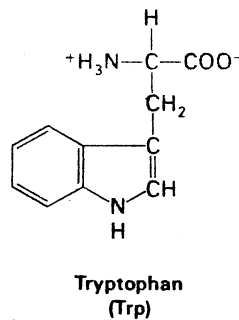
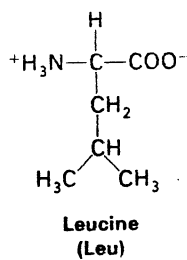
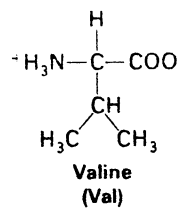
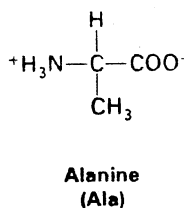
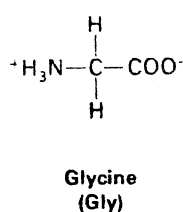
## APPENDIX A

## CHEMICAL STRUCTURE OF GRAMICIDIN A

The chemical structure of gramicidin A is :



which consists of 15 hydrophobic amino acids of alternating *L* and *D* isomers. The N-terminus is blocked by a formyl group ( HCO- ) and the C-terminus by an ethanolamine group ( -NHCH<sub>2</sub>CH<sub>2</sub>OH ). The five amino acids are diagrammed below :



## APPENDIX B

TRANSLATING THE ORDER PARAMETER  $S_n$  FROM THE  
EXPERIMENTAL QUADRUPOLE SPLITTING DATA

The experimental quadrupole splitting  $\Delta\nu$  is produced by deuterium NMR spectra. The deuterium order parameter  $S_{CD}$  of the C-D bond can be calculated according to [42]

$$\Delta\nu = (3/4)(e^2qQ/h)S_{CD}, \quad (61)$$

where the deuteron quadrupole splitting constant  $(e^2qQ/h) \approx 170$  kHz for paraffin chains [9]. The definition of  $S_{CD}$  is given by

$$S_{CD} = (1/2)(3 \langle \cos^2 \beta \rangle - 1) \quad (62)$$

where  $\beta$  is the angle between the CD bond and the magnetic field (chosen along the bilayer normal). Because the average CD bond is basically perpendicular to the bilayer normal ( $\beta \approx \pi/2$ ),  $S_{CD}$  is negative.  $S_{CD}$  can be approximately related to the segmental order parameter  $S_{mol}$  [41]

$$S_{mol} = -2S_{CD}. \quad (63)$$

Substituting Eq.(62) in Eq.(63), the amplitude of  $S_{mol}$  is

$$\begin{aligned} |S_{mol}| &= \frac{8}{3 \times 170} \\ &= 0.0157\Delta\nu. \end{aligned} \quad (64)$$

In this study, the order-parameter profile  $S_n$  can be compared with the experimental data  $S_{mol}$ . The experiment data should be uniformly divided by 0.5 to approximately correct for localized chain titling, [39]. the titling is not considered in this simulation, so

$$\begin{aligned} S_n &= |S_{mol}|/0.5 \\ &= 0.0314\Delta\nu, \end{aligned} \quad (65)$$

by which all experimental data are translated to  $S_n$ .

VITA

JIAN XING

Candidate for the Degree of

Master of Science

Thesis: 3-DIMENSIONAL MONTE CARLO SIMULATION OF LIPID-GRAMICIDIN A INTERACTION IN MODEL MEMBRANES

Major Field: Physics

Biographical:

Personal Data: Born in Chengdu, Sichuan, P. R. China, March 24, 1954, the son of Yu-Ting Xing and Shao-Kun Yang.

Education: Graduated from the 29th Middle School, Chengdu, Sichuan, P. R. China, in May, 1971; received Bachelor of Science Degree in Physics from Sichuan University, Chengdu, Sichuan, P. R. China in August 1982; completed the requirements for the Master of Science Degree at Oklahoma State University in July, 1989.

Professional Experience: Research Assistant, Analytic Center, Steel Company, Chengdu, Sichuan, P. R. China, Jan. 1976 to Sep. 1978; Undergraduate Research Assistant, Sichuan University, Chengdu, Sichuan, P. R. China, Sep. 1981 to Aug. 1982; Researcher, Institute of Optics and Electronics, Chinese Academy of Sciences, Sep. 1982 to Apr. 1985; Technical Service Engineer, China Service Center of BAIRD Corporation (USA), Apr. 1985 to Feb. 1987; Graduate Research Assistant, Oklahoma State University, Jun. 1988 to present.